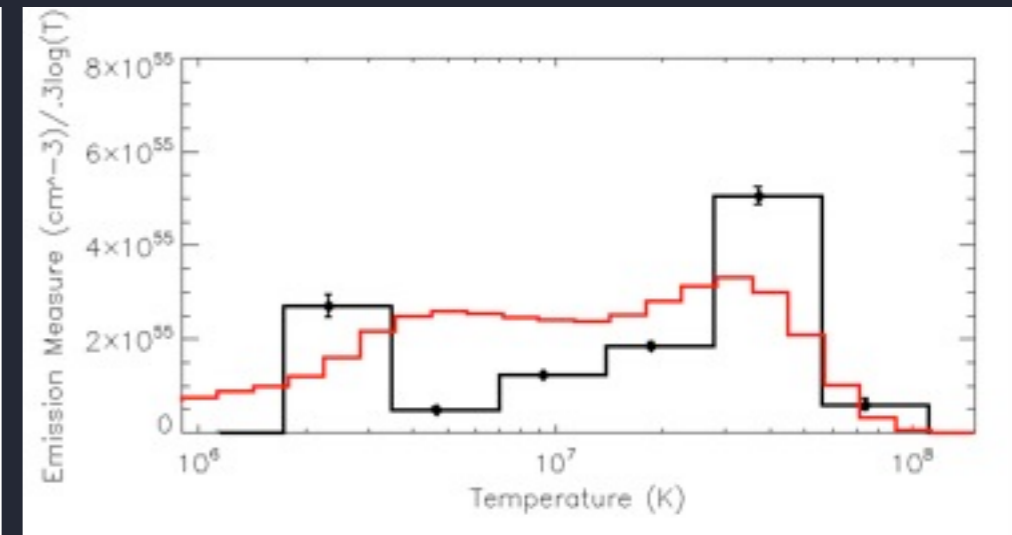
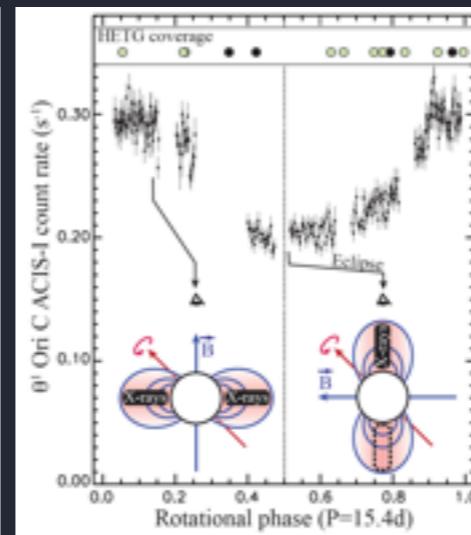
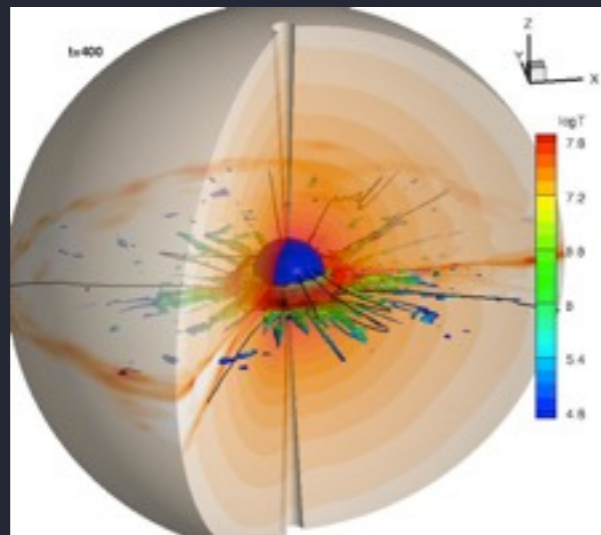
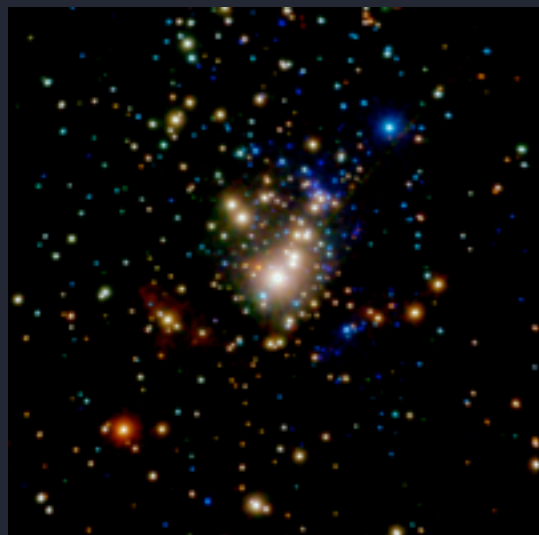


New X-ray Observations and Numerical Modeling of the Prototype Magnetic O Star θ^1 Ori C

David Cohen
Department of Physics & Astronomy
Swarthmore College

Asif ud-Doula, Véronique Petit, Stan Owocki, Maurice Leutenegger, Marc Gagné, Rich Townsend, Gregg Wade, Alex Fullerton, Jon Sundqvist, and Jackie Pezzato (Swarthmore '17) and Randy Doyle (Swarthmore '16)



Physics & Astronomy @ Swarthmore College

Swarthmore College

ALUMNI | CAMPUS COMMUNITY | PARENTS | VISITORS

 Search ▶

A-Z INDEX | CALENDAR | CONTACTS

Peter van de Kamp Observatory

Home

About

Academics

Admissions & Aid

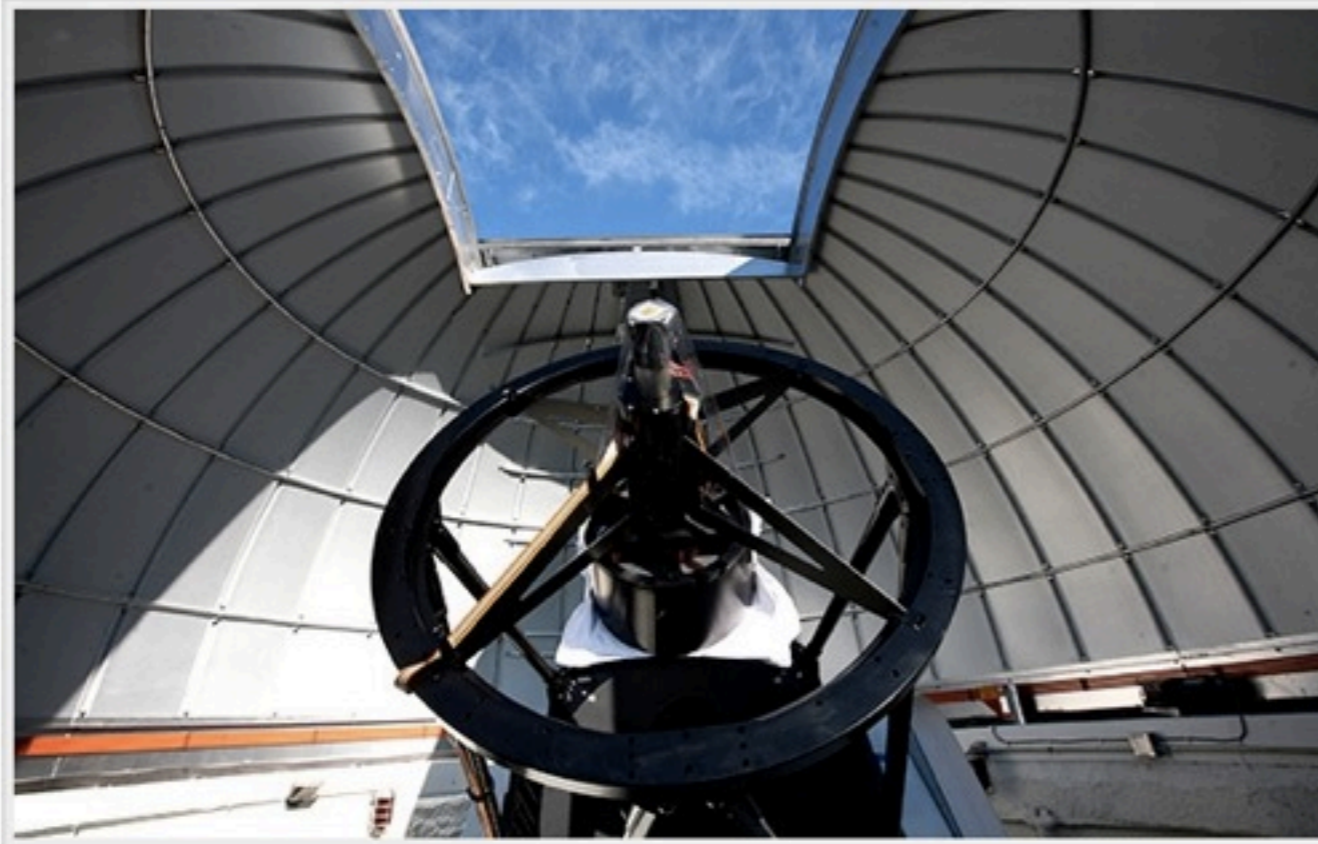
Athletics

Giving

Libraries

News & Events

Student Life



The Peter van de Kamp Observatory atop the Science Center at Swarthmore College houses a 24-inch telescope with a suite of imaging, photometric, and spectroscopic instrumentation. It is used by Swarthmore faculty, staff, and students for research, teaching, and outreach and is open to the public the second Tuesday of each month.

Astronomy professors [Eric Jensen](#) and [David Cohen](#) use the telescope in their research on exoplanets, young stars, and massive stars. Swarthmore students participate in these projects, and students in classes ranging

Peter van de Kamp Observatory

[Technical Capabilities](#)

[Research](#)

[Course and Lab Work](#)

[Public Viewing](#)

[Directions](#)

Physics & Astronomy



The [Physics & Astronomy Department](#) offers a wide variety of classes, including an ambitious curriculum of advanced seminars for our physics and astrophysics majors, as well as many introductory classes for all students. As befits a department of scientists with a strong liberal arts outlook, these

Physics & Astronomy @ Swarthmore College

Swarthmore College

ALUMNI | CAMPUS COMMUNITY | PARENTS | VISITORS

Search ▶

A-Z INDEX | CALENDAR | CONTACTS

Peter van de Kamp Observatory

Home

About

Academics

Admissions & Aid

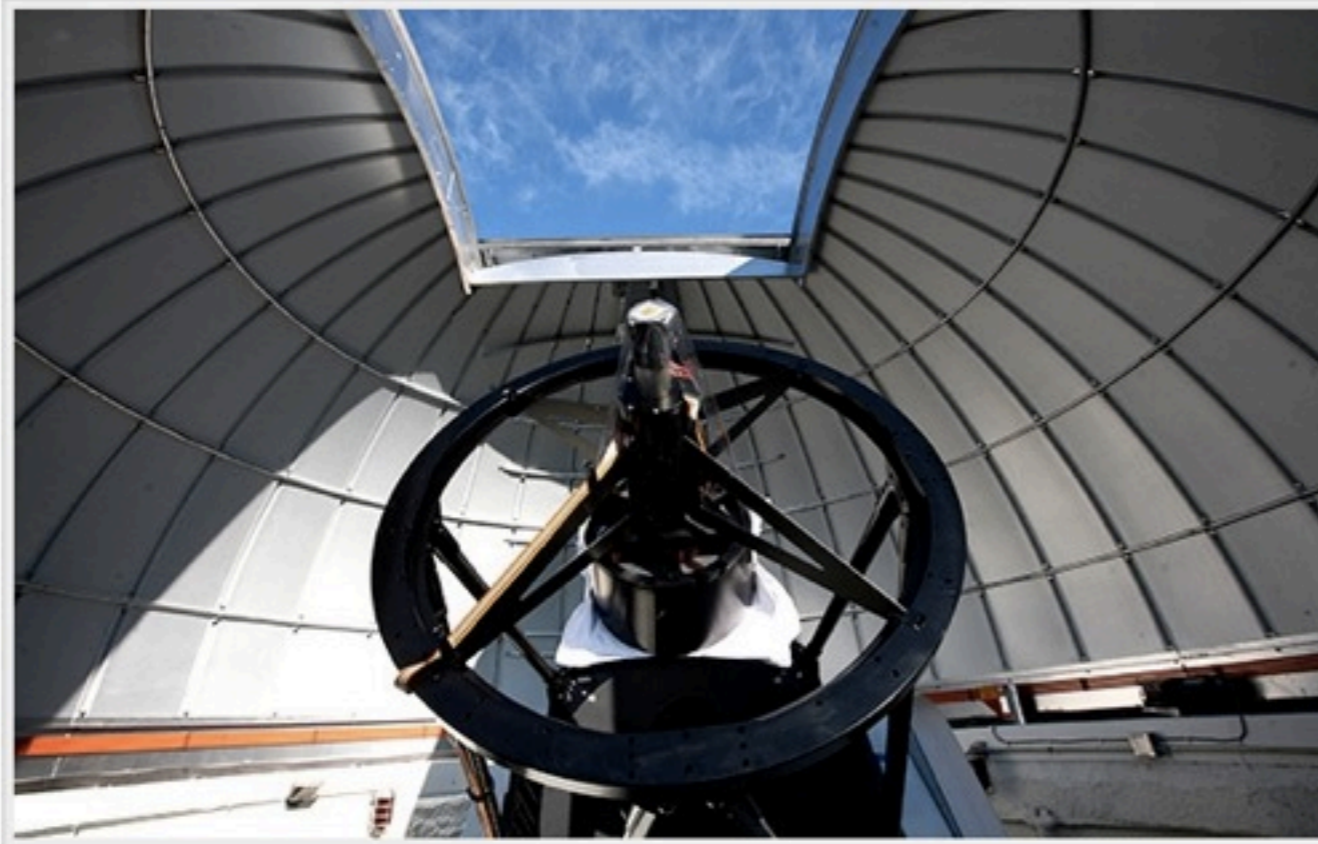
Athletics

Giving

Libraries

News & Events

Student Life



The Peter van de Kamp Observatory atop the Science Center at Swarthmore College houses a 24-inch telescope with a suite of imaging, photometric, and spectroscopic instrumentation. It is used by Swarthmore faculty, staff, and students for research, teaching, and outreach and is open to the public the second Tuesday of each month.

Astronomy professors [Eric Jensen](#) and [David Cohen](#) use the telescope in their research on exoplanets, young stars, and massive stars. Swarthmore students participate in these projects, and students in classes ranging

Peter van de Kamp Observatory

[Technical Capabilities](#)

[Research](#)

[Course and Lab Work](#)

[Public Viewing](#)

[Directions](#)

Physics & Astronomy



The [Physics & Astronomy Department](#) offers a wide variety of classes, including an ambitious curriculum of advanced seminars for our physics and astrophysics majors, as well as many introductory classes for all students. As befits a department of scientists with a strong liberal arts outlook, these

Peter van de Kamp
director, Sproul Observatory
Swarthmore College
(1937-1972)

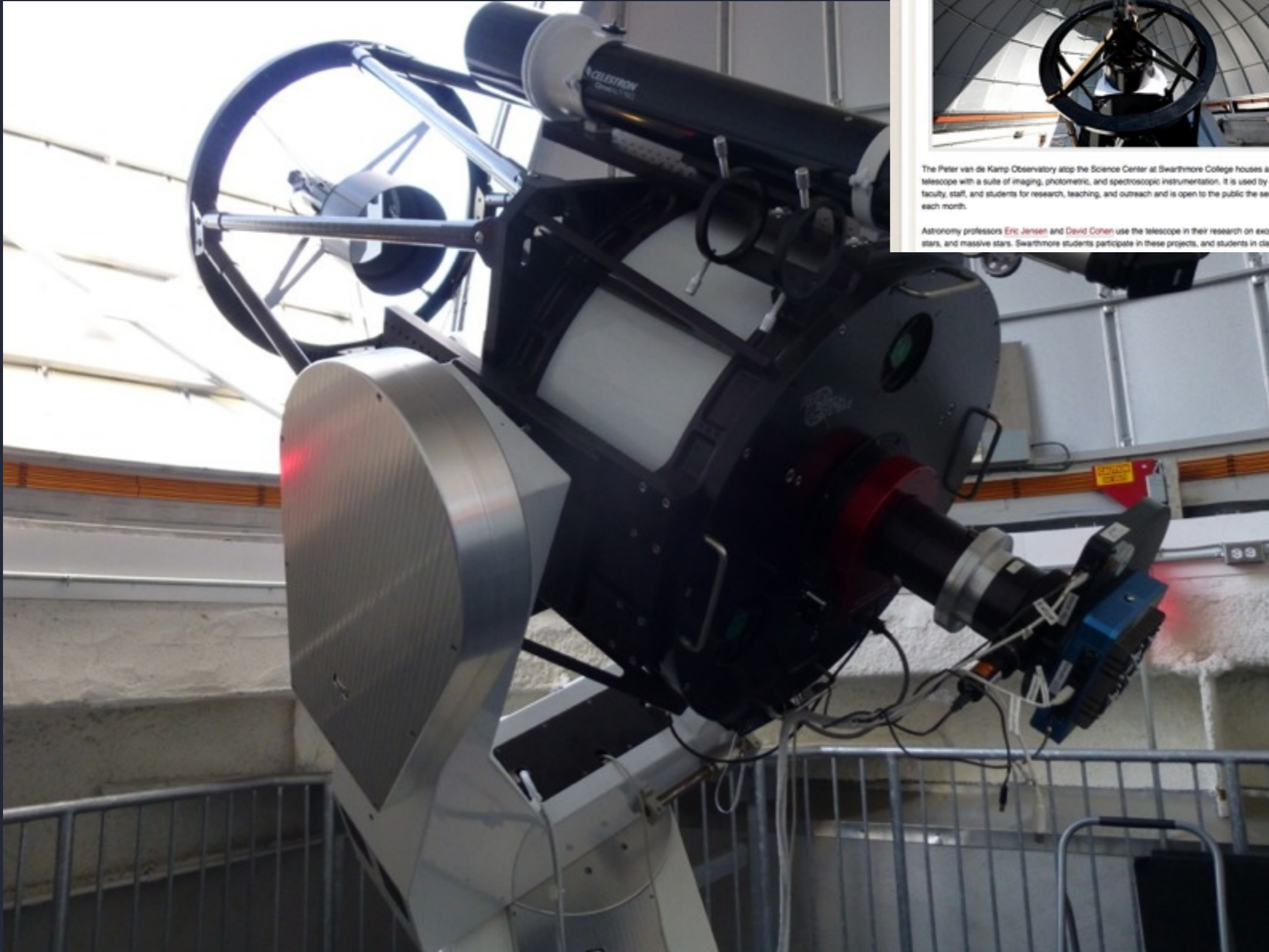


Sproul Observatory
Swarthmore College
(1912)

24-inch refractor (f/17)



Peter van de Kamp Observatory established 2009



Swarthmore College

ALUMNI | CAMPUS COMMUNITY | PARENTS | VISITORS

Search

A-Z INDEX | CALENDAR | CONTACTS


Peter van de Kamp Observatory

Home About Academics Admissions & Aid Athletics Giving Libraries News & Events Student Life

Peter van de Kamp Observatory

- Technical Capabilities
- Research
- Course and Lab Work
- Public Viewing
- Directions

Physics & Astronomy



The **Physics & Astronomy Department** offers a wide variety of classes, including an ambitious curriculum of advanced seminars for our physics and astrophysics majors, as well as many introductory classes for all students. As befits a department of scientists with a strong liberal arts outlook, these

The Peter van de Kamp Observatory atop the Science Center at Swarthmore College houses a 24-inch telescope with a suite of imaging, photometric, and spectroscopic instrumentation. It is used by Swarthmore faculty, staff, and students for research, teaching, and outreach and is open to the public the second Tuesday of each month.

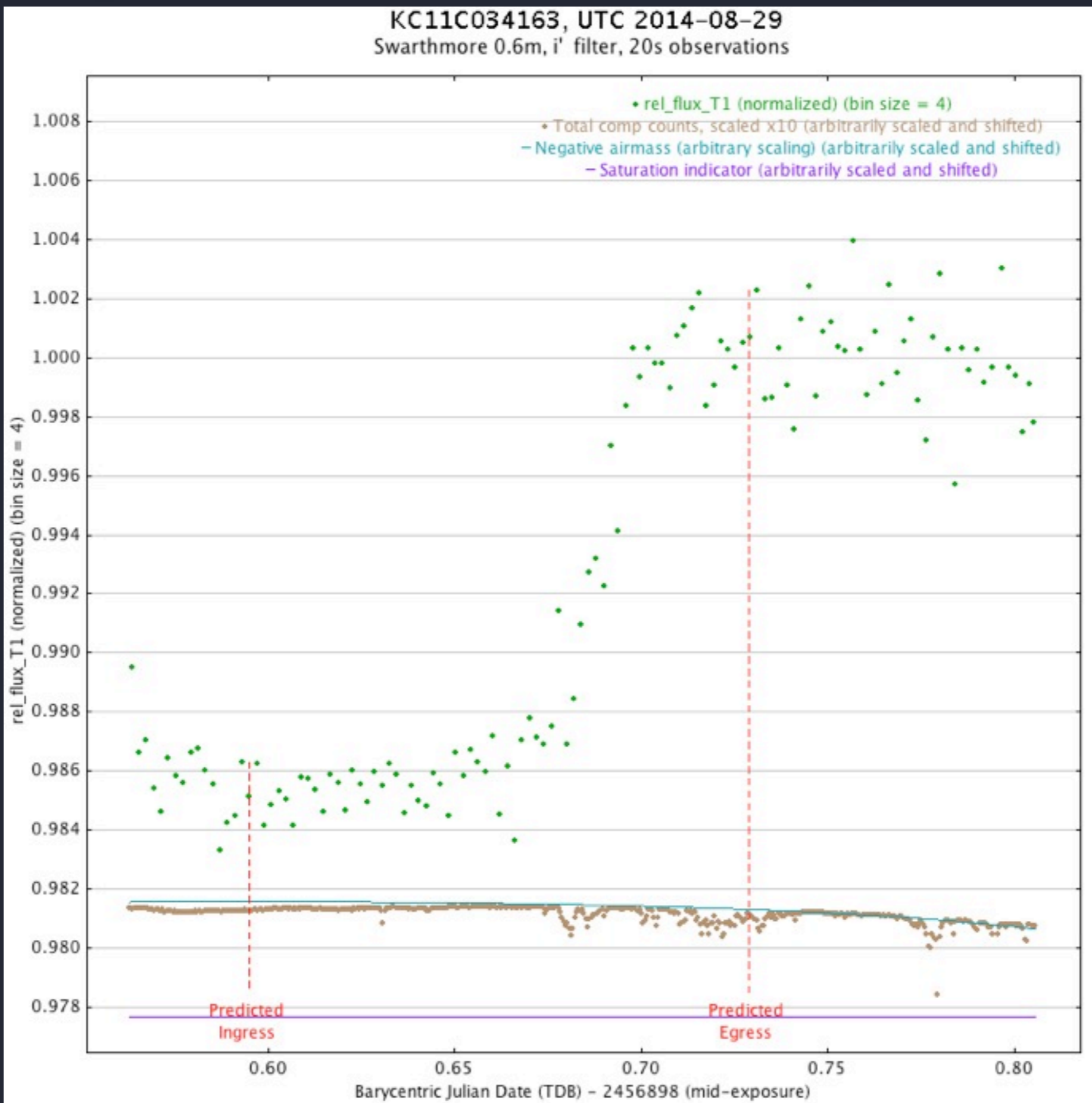
Astronomy professors **Eric Jensen** and **David Cohen** use the telescope in their research on exoplanets, young stars, and massive stars. Swarthmore students participate in these projects, and students in classes ranging

Physics & Astronomy @ Swarthmore College

24-inch (0.61 m) RCOS telescope: mostly
exoplanet transit photometry



exoplanet transit candidate: ~1 mmag precision



2011 visit to UvA:APO



it's windy on the roof



nearly the same set-up as PvdK Observatory



Principles of Astrometry

With Special Emphasis on
Long-Focus Photographic Astrometry

PETER VAN DE KAMP

Sprout Observatory, Swarthmore College

This textbook, written by a leading authority in the field, is the first general introduction to the theory, technique, reduction methods, and results of astrometry, particularly of long-focus photographic astrometry.

Astrometry is the branch of astronomy that deals with measurements of the celestial bodies involving their positions and movements. The subject has always been a fundamental one in astronomy but has assumed renewed importance in this day of space vehicles. Although it is covered extensively in research papers and compendia, there has heretofore been no general introduction to the subject.

The level of the book is intermediate; an introductory knowledge of astronomy and an understanding of solid geometry, trigonometry, and calculus are assumed. In addition to its use as a text in courses in astrometry, the book will prove useful in courses dealing with the stars, galactic structure, spherical astronomy, practical astronomy, proper motions and parallaxes, descriptive astronomy (if on a sufficiently advanced level), celestial mechanics, and orbit determinations.

Van de Kamp

Koninklijke Academie van Wetenschappen, Amsterdam, 1974. **Prix Janssen** uitgereikt aan de Nederlandse sterrenkundige Peter van de Kamp. Deze hoogste Franse onderscheiding op astronomisch gebied wordt sedert 1897 eens per jaar toegekend door de Société Astronomique de France. Peter van de Kamp werd in 1901 in Kampen geboren. Na zijn wis- en natuurkundestudie aan de Universiteit van Utrecht vertrok hij

1982
na hij directeur van de Sprout sterrenwacht en hoogleraar in de sterrenkunde aan het Swarthmore College in Pennsylvania. Van de Kamp is vooral bekend geworden door zijn jarenlange onderzoek, dat hem tot de conclusie bracht dat rond de ster van Barnard twee planeten draaien. Daarvoor werden alleen bekend was dat onze eigen zon door planeten omringd is, werd Van de Kamp ontdekkende als

alle recht maken!



Pvdk

Peter van de Kamp
1974 Oct 28
Amsterdam

Magnetism and Variability in O Stars

the look of a prophet

Magnetism and variability in O stars

Cassiopeia

Perseus

λ

γ

β Cepheus

Amsterdam

17-19 September 2014

Magnetism and Variability in O Stars

C IV DAC... I think I see a magnetic field



Magnetism and variability in O stars

λ Cepheus β Cassiopeia γ Perseus ξ

Amsterdam
17-19 September 2014

Magnetism and Variability in O Stars

the mature scientist: ...now
we've measured it

Magnetism and variability in O stars

Cassiopeia

Perseus

λ

γ

β Cepheus

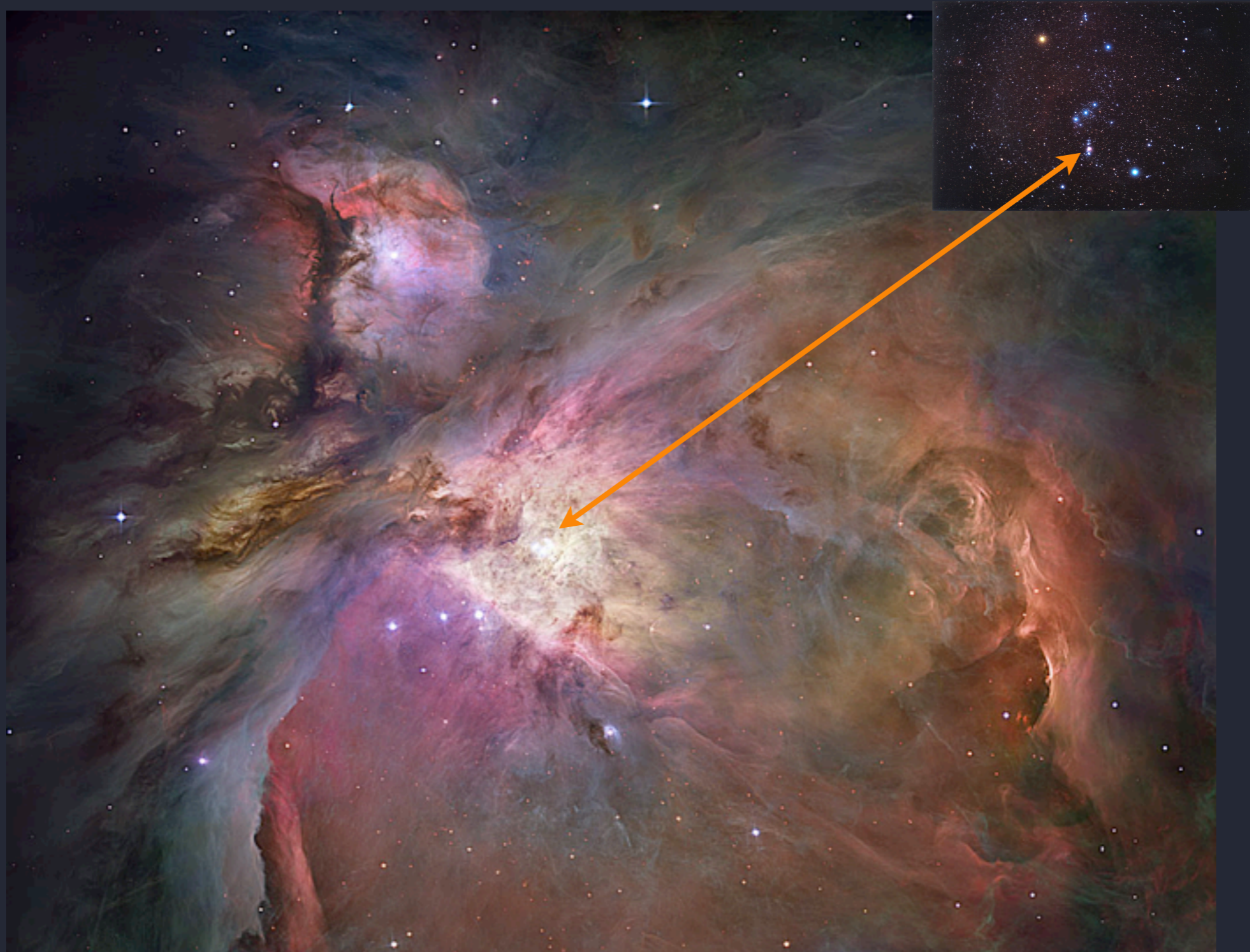
Amsterdam

17-19 September 2014

Outline/overview:

$$L/L_{\text{sun}} = 10^{5.4}$$
$$\dot{M} \sim 5 \times 10^{-7} M_{\text{sun}}/\text{yr}$$

θ^1 Ori C is a young (< 1 Myr) O7 star





Orion Nebula Cluster - *Chandra* color-coded by X-ray hardness

θ^1 Ori C: the strongest X-ray source in the cluster



θ^1 Ori C is a magnetic O star prototype:
tilted dipole, confined magnetosphere

$$i \sim \beta \sim 45^\circ$$

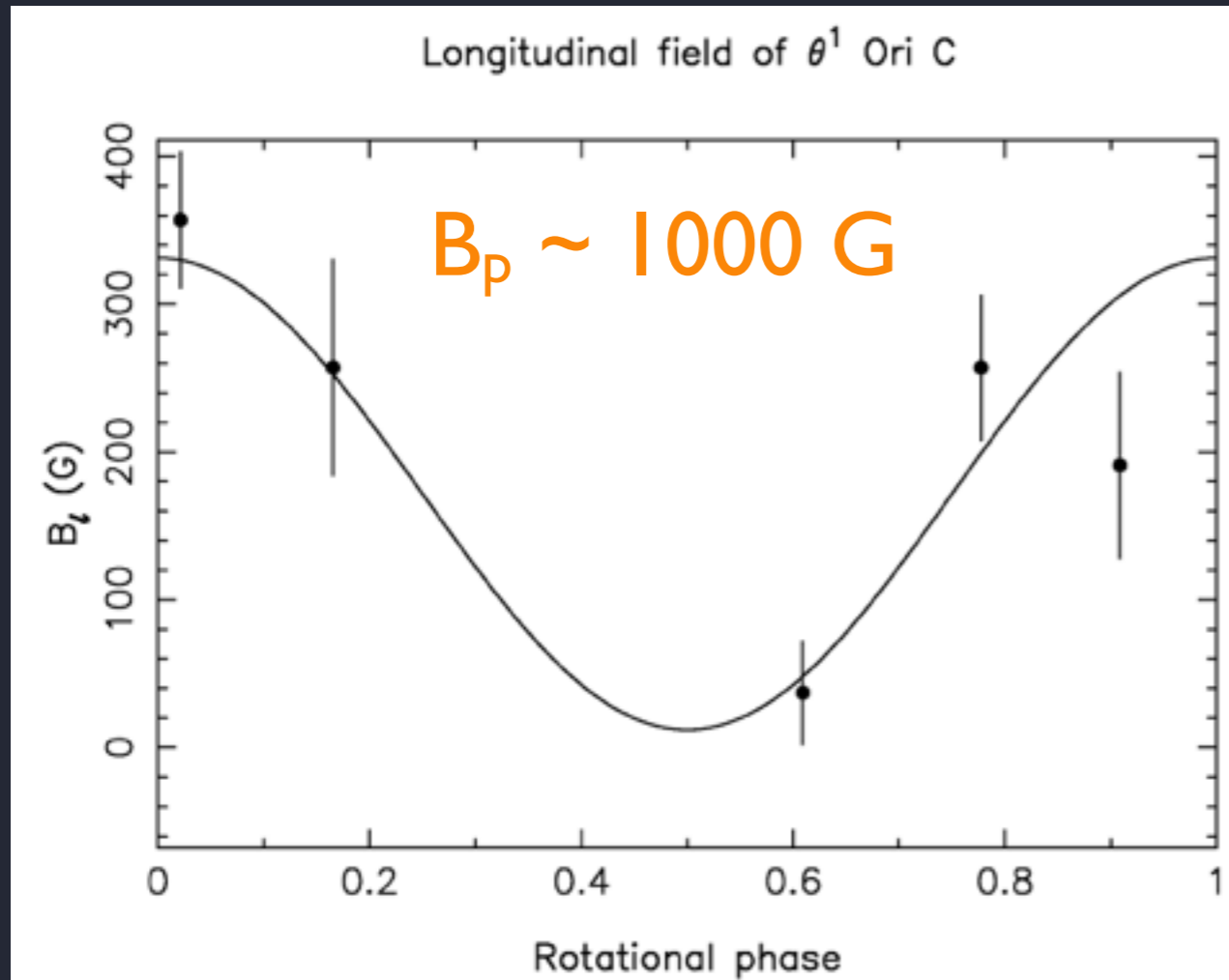
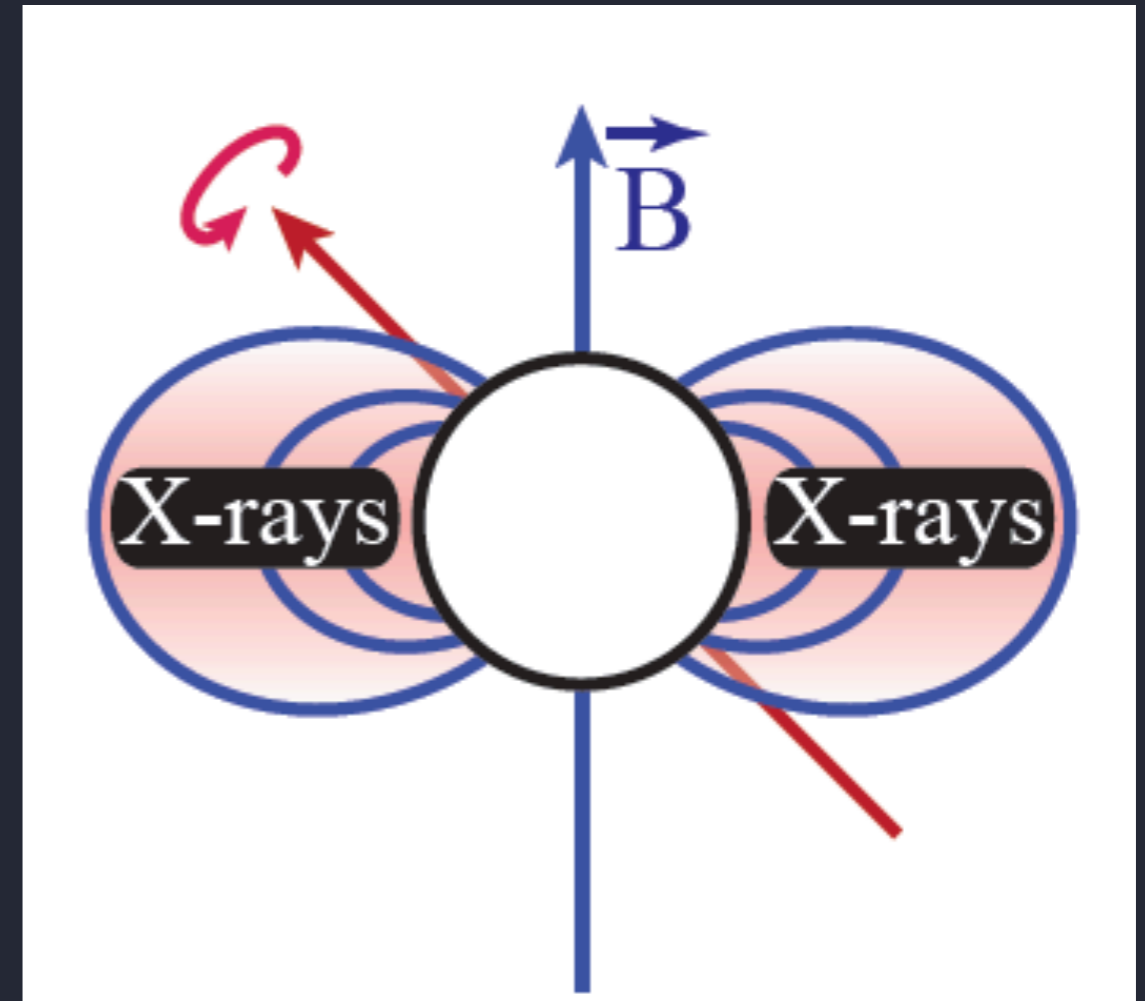


Figure 2. Longitudinal field estimates (filled circles) and error bars derived from our five mean LSD Stokes profiles, as a function of rotational phase (using the ephemeris of Stahl 1998). The full line depicts the least-squares cosine fit to the data.

© 2002 RAS, MNRAS 333, 55–70

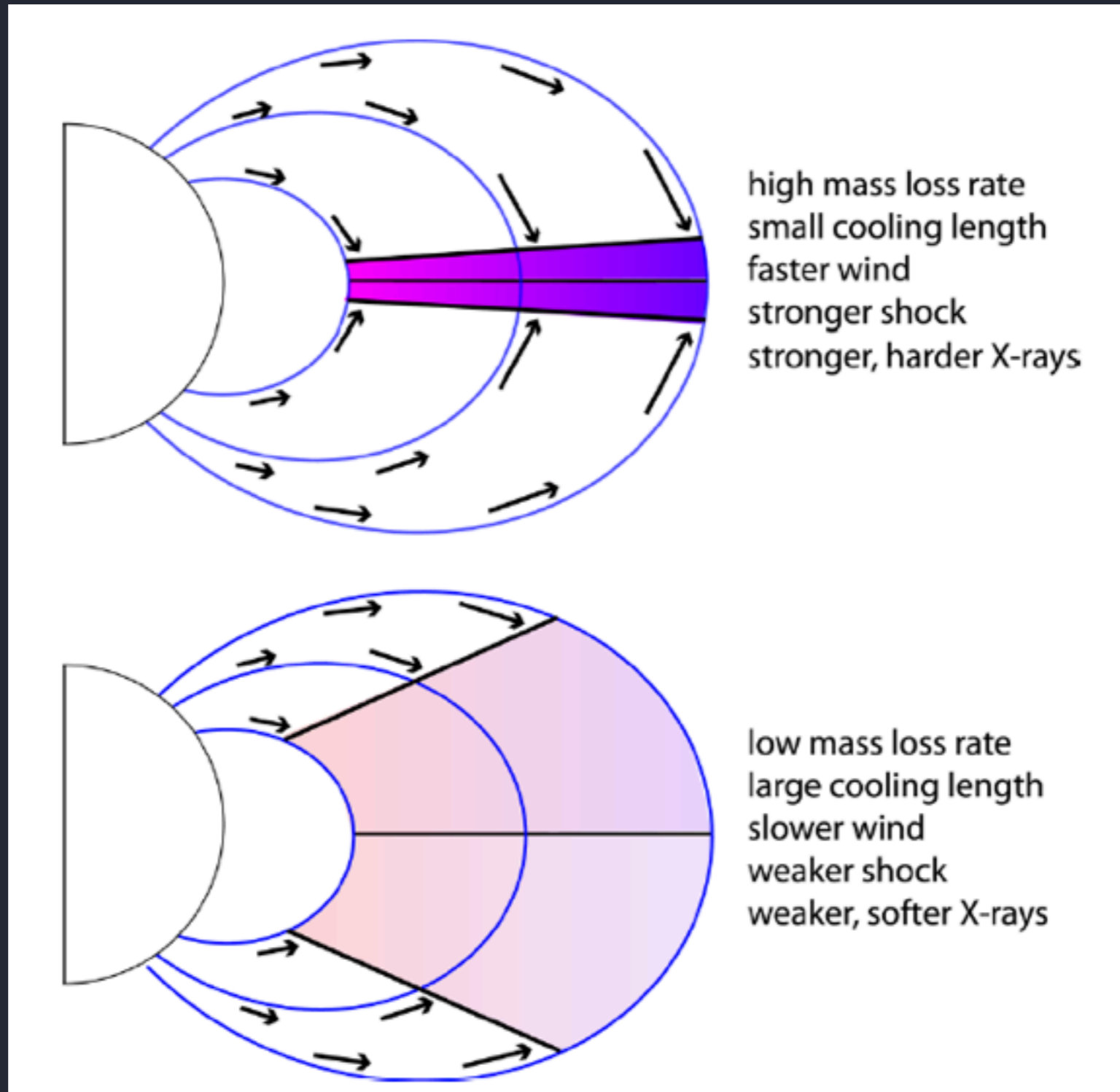
Donati et al. 2002



X-rays trace the dissipation of wind KE in the magnetosphere

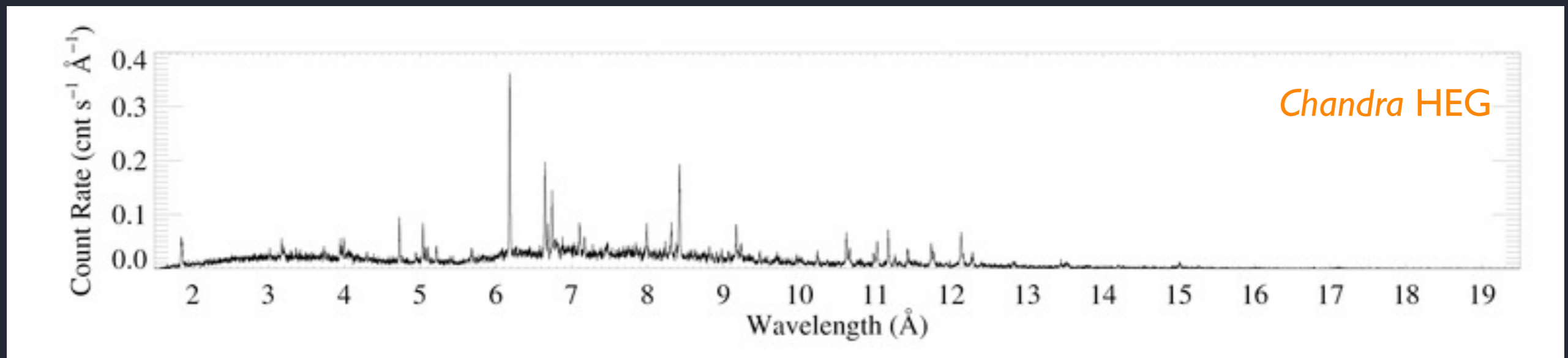
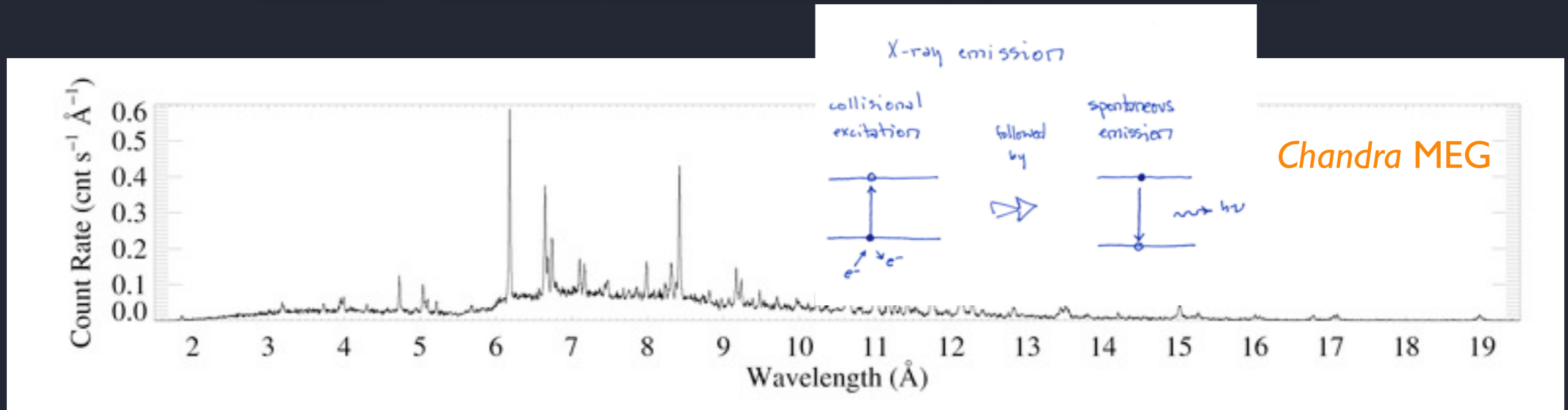
Plasma heating from hydrodynamic shocks

wind kinetic energy converted to heat: $T \sim 10^6 (v_{\text{shock}}/300 \text{ km/s})^2 \text{ K}$



X-rays are optically thin line emission

“coronal” = collisional excitation followed by spontaneous emission

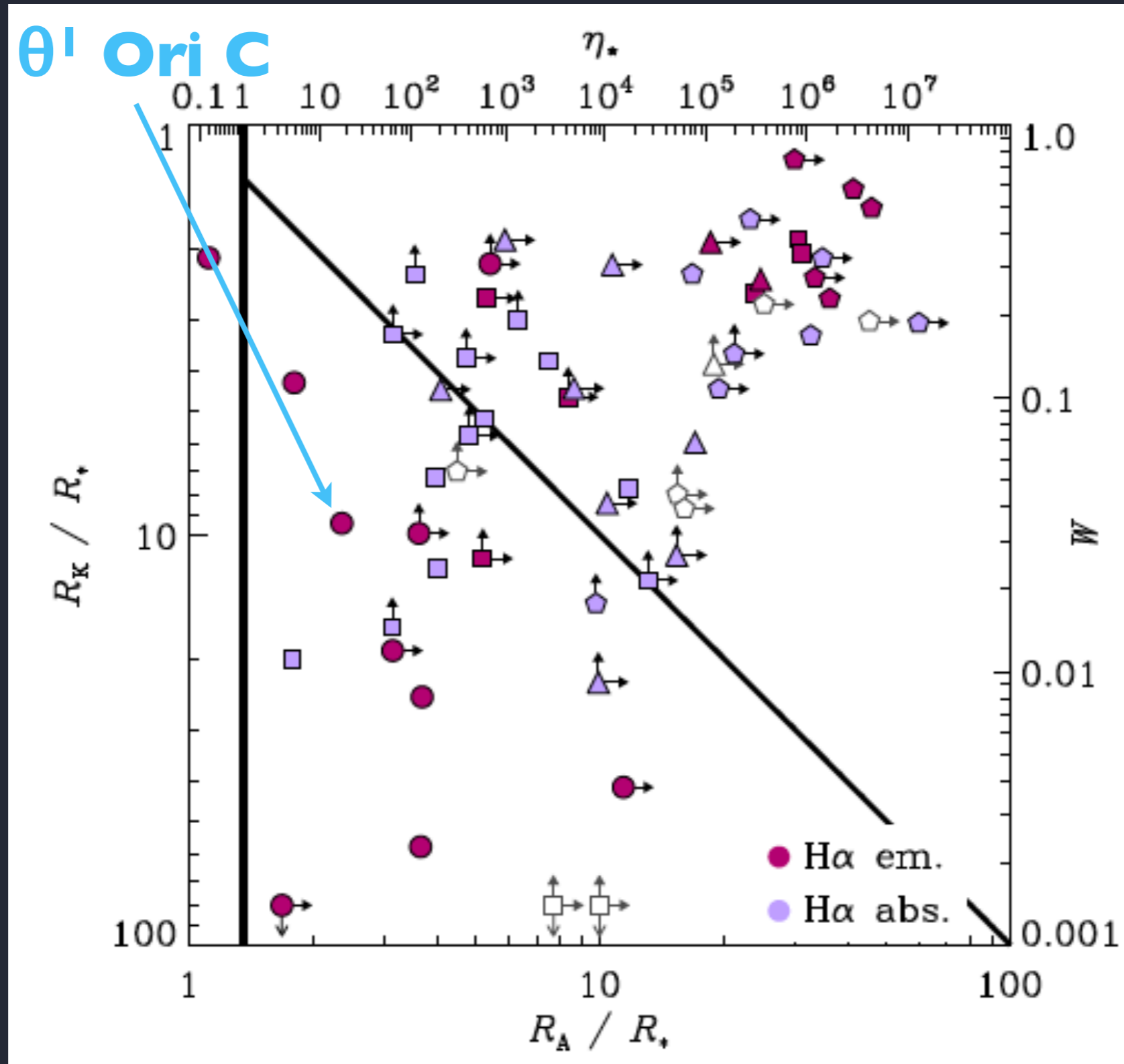


relative line strengths are dependent on **temperature** and **abundance**, primarily

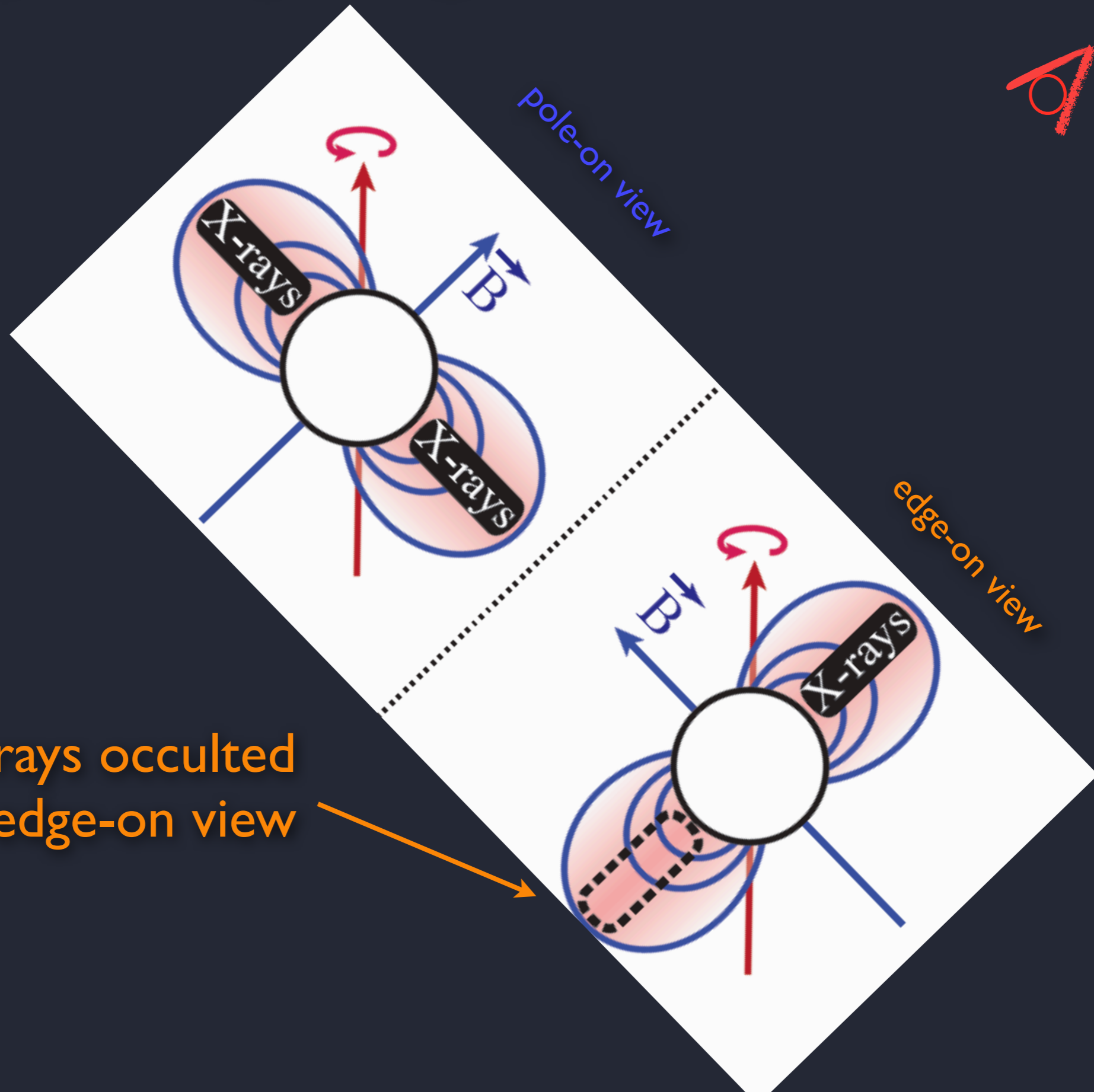
θ^1 Ori C is a slow rotator, moderate confinement ($\eta_* \sim 20$) = DM (dynamical magnetosphere); no centrifugal support

confinement \longrightarrow

rotation (Kepler radius) \uparrow

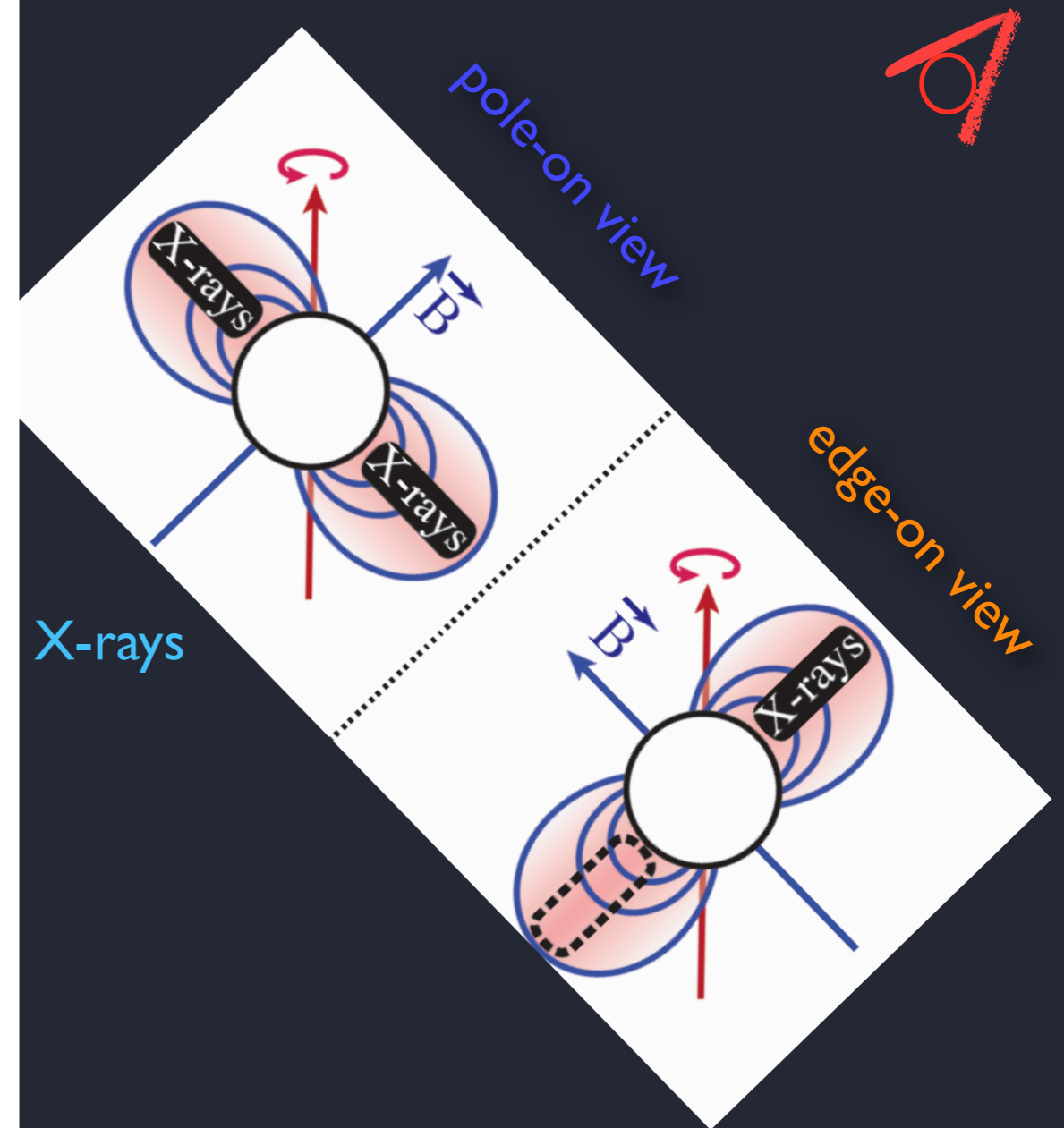
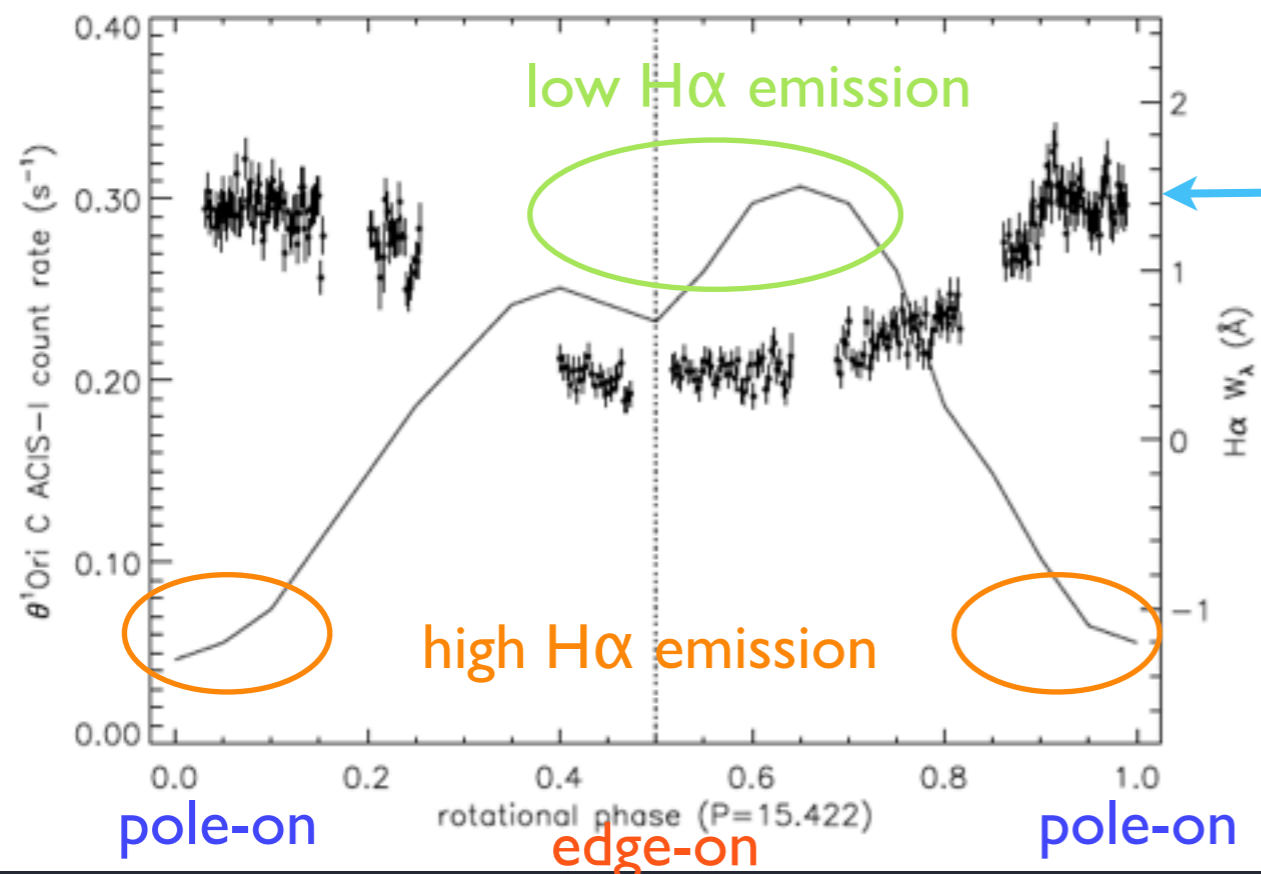
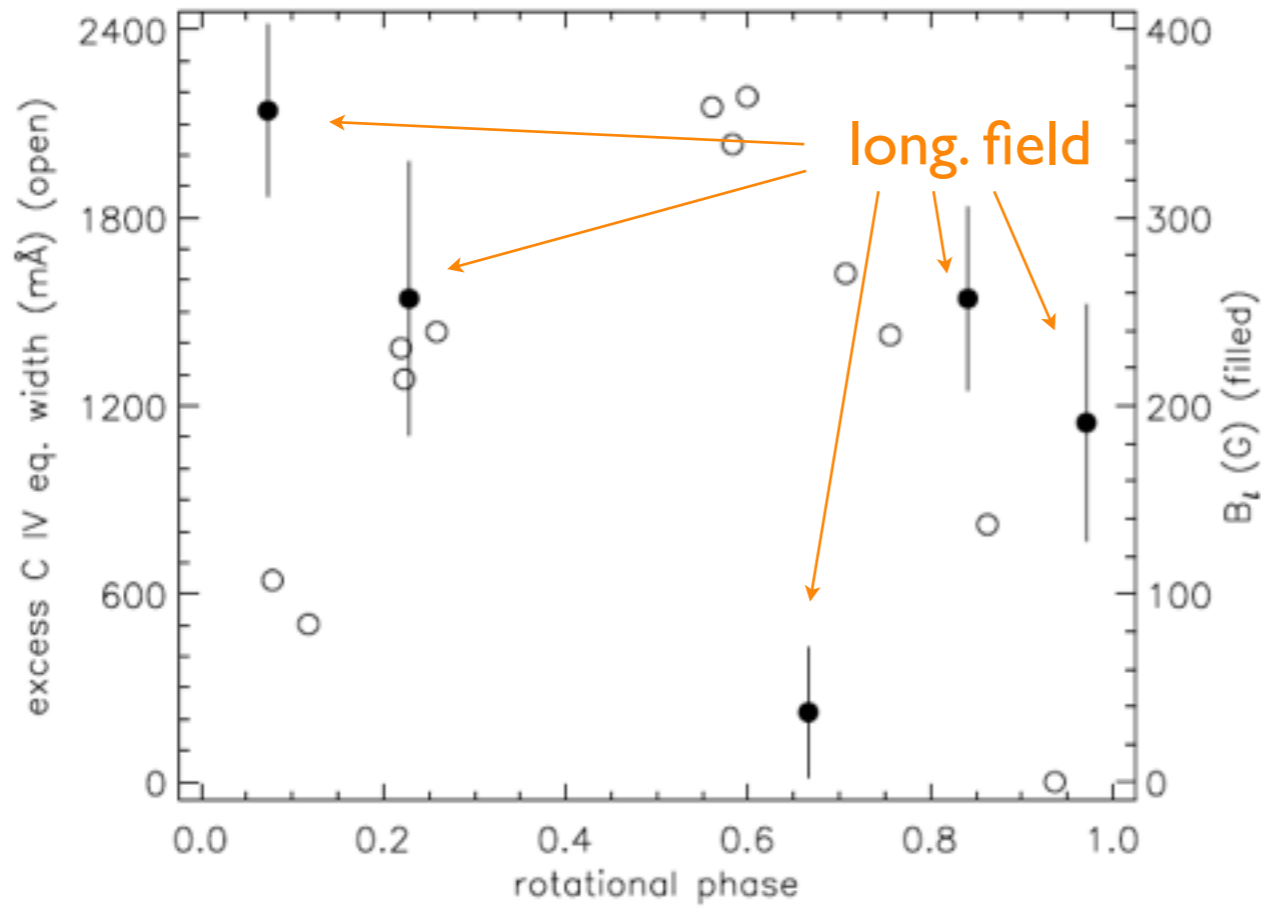


tilted dipole: oblique magnetic rotator



some X-rays occulted
in edge-on view

tilted dipole: oblique magnetic rotator



V. Petit

Goals: use multiwavelength diagnostics and rotational modulation to probe the physical properties of the magnetosphere, the shock-physics, the wind mass-loss rate...and constrain numerical simulations

MHD simulations: 2-D, hemispherical slice

density

temperature

X-ray emission

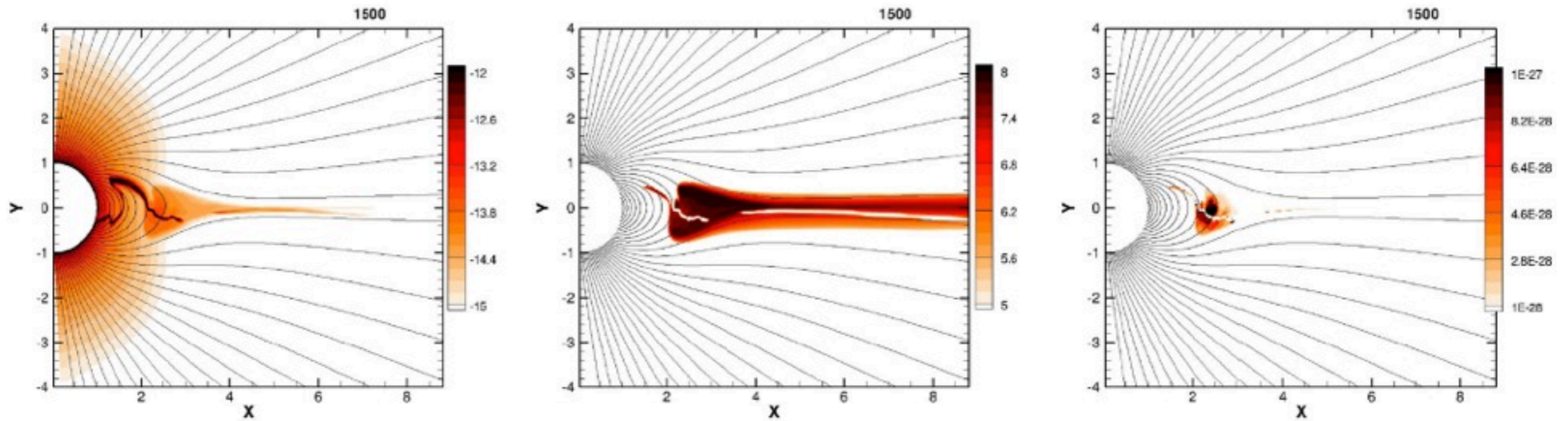
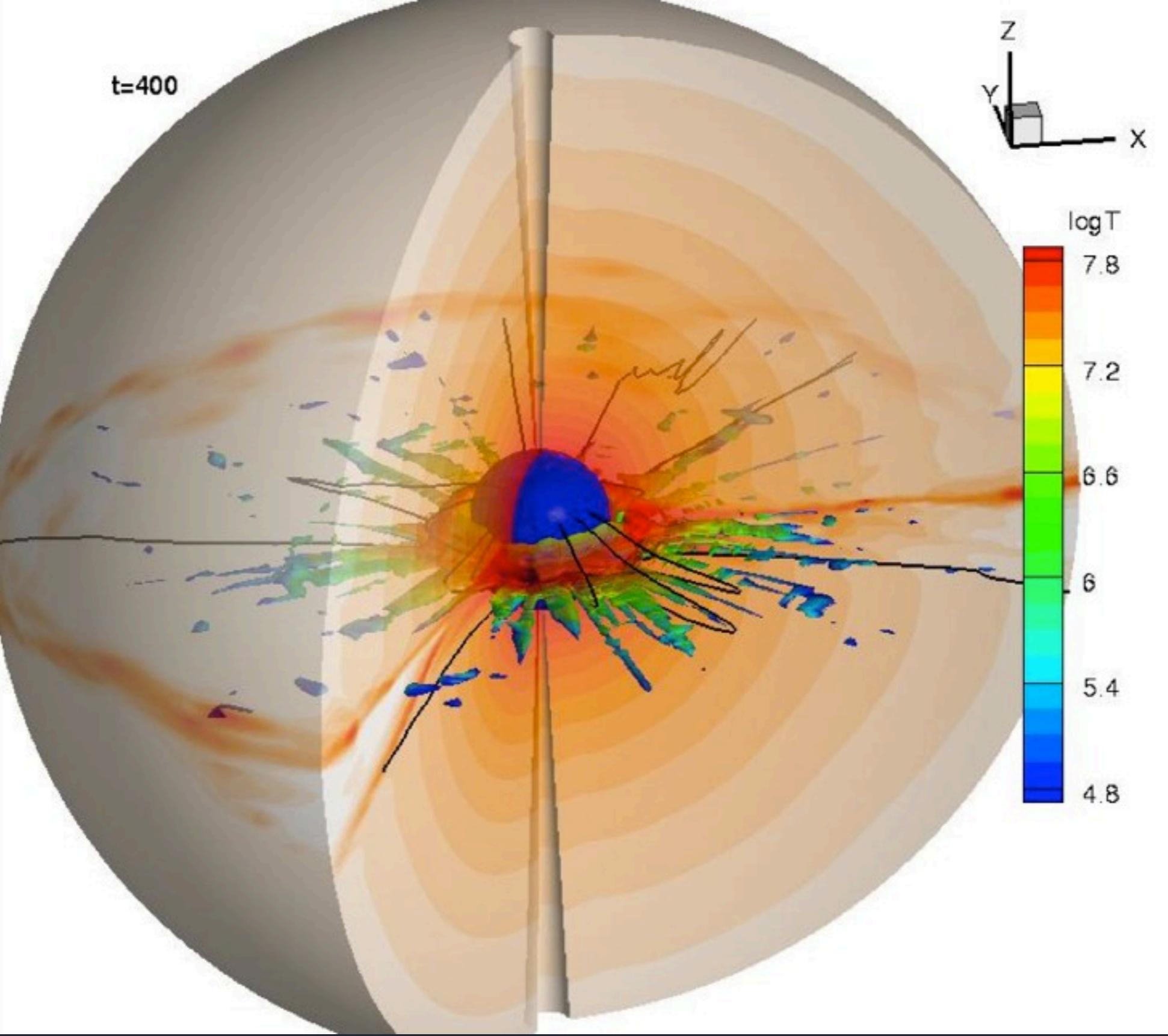


Figure 4. Colour plots of log density (left) and log temperature (middle) for arbitrary snapshot of structure in the standard model with $\eta_* = 100$ and no IC cooling. The right-hand panel plots the proxy X-ray emission XEM_{T_x} (weighted by the radius r) from (26), on a *linear* scale for a threshold X-ray temperature $T_x = 1.5$ MK.

ud-Doula et al. 2014

3-D MHD simulation: log Temperature

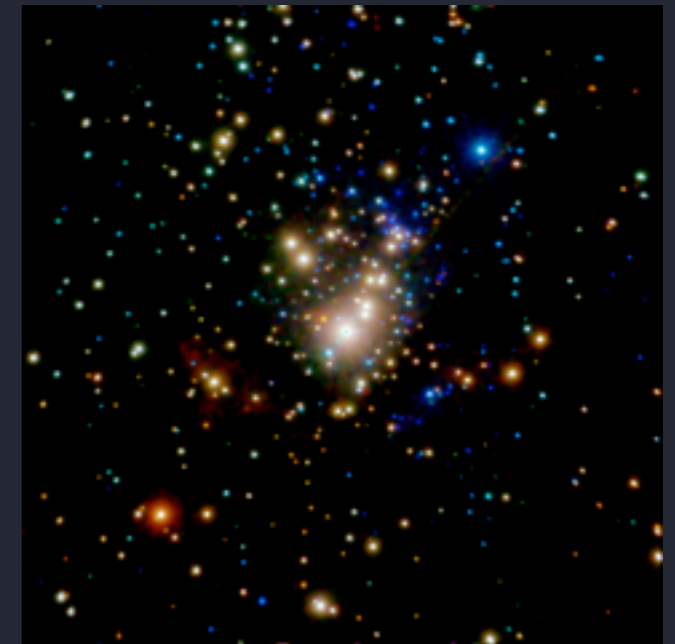


from A. ud-Doula

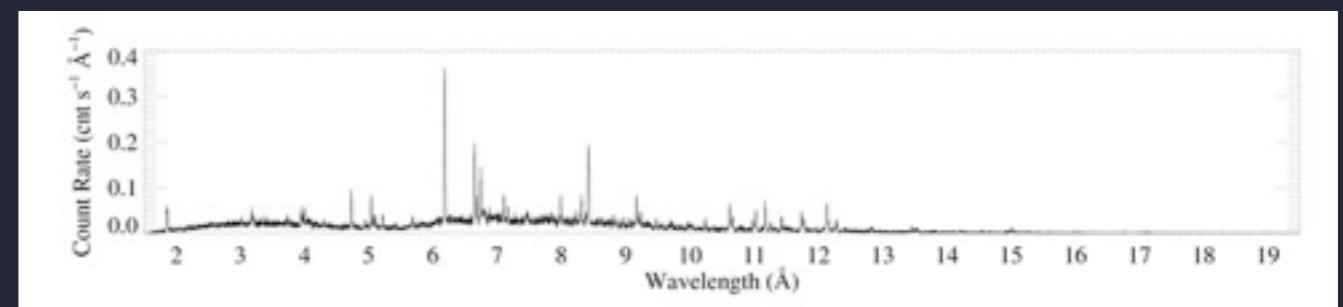
Chandra



Orion Nebula Cluster - Chandra



Chandra grating spectroscopy



response to photons with $h\nu \sim 0.5$ keV up to a few keV
(corresp. $\sim 5\text{\AA}$ to 24\AA)

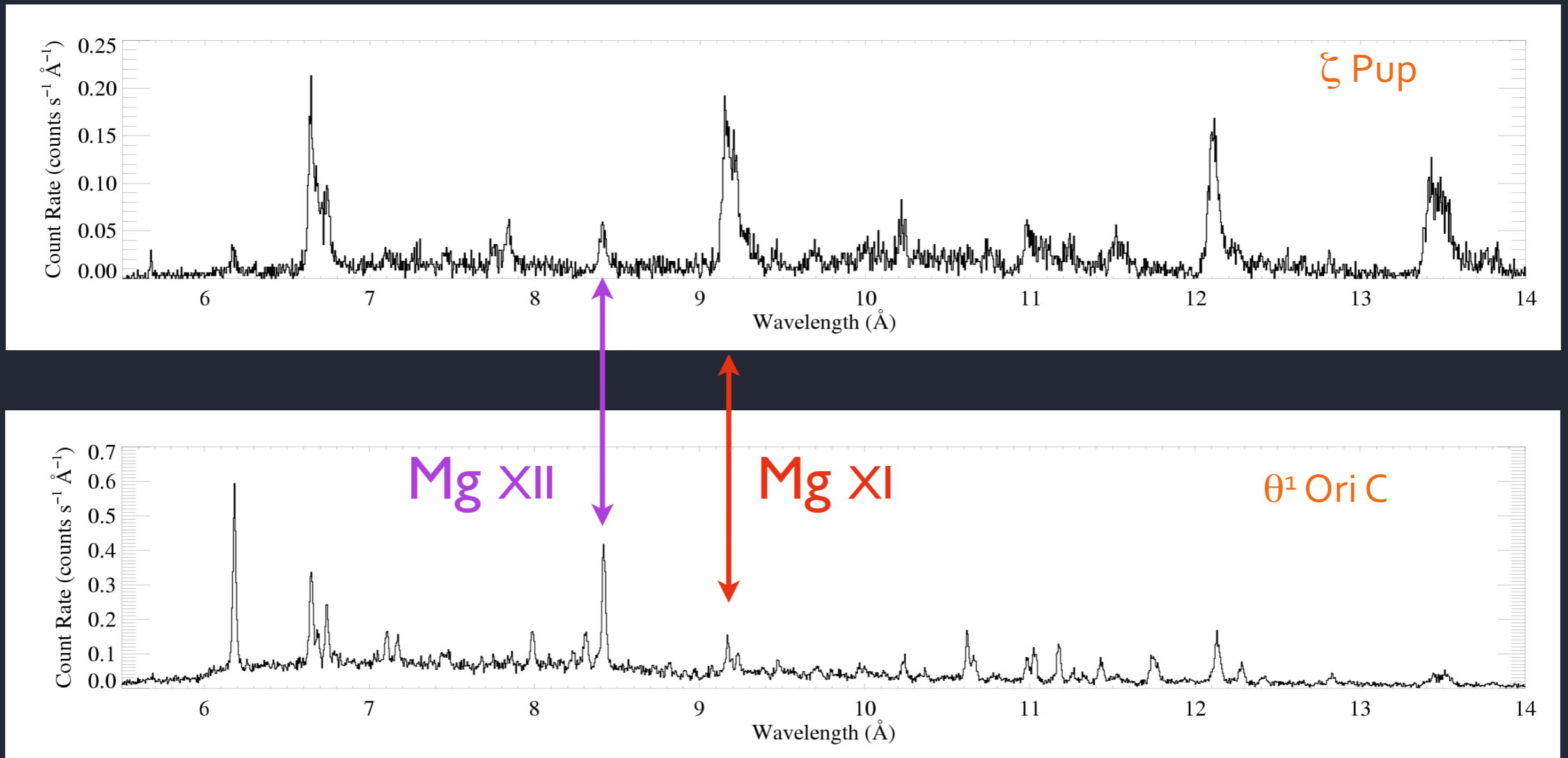
spectroscopy ($R < 1000$ corresp. >300 km/s)

small effective area (poor sensitivity)
but very low background and very well calibrated

$kT = h\nu$ gives
 $T \sim 12 \times 10^6$ K
for 1 keV

Line ratios as temperature indicators

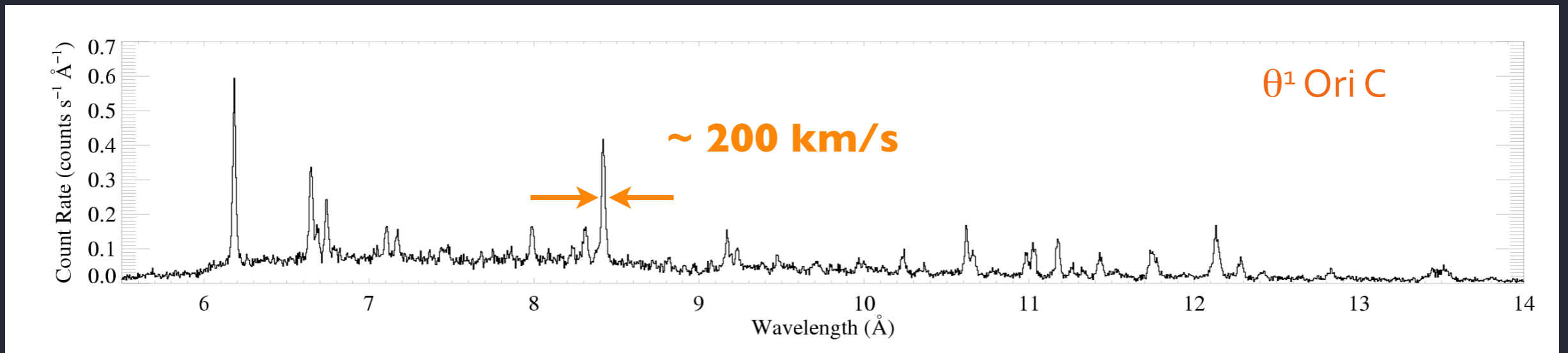
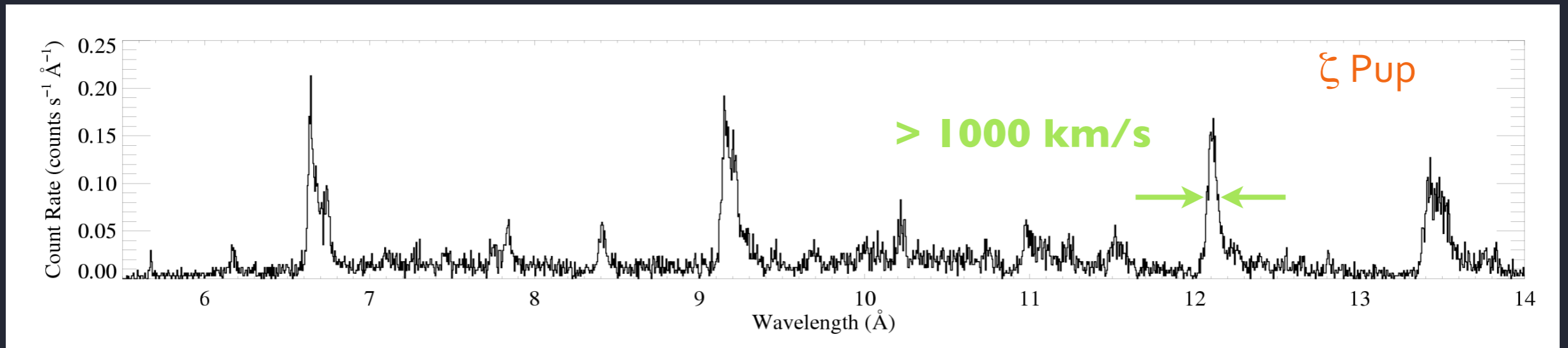
Mg XII / Mg XI is proportional to temperature



Chandra spectra of prototype non-magnetic (zeta Pup, top) and magnetic (θ^1 Ori C, bottom) stars

Line widths from gas kinematics

non-magnetic O stars: $v_{\text{line}} \sim v_{\text{wind}}$ but MCWS: $v_{\text{line}} < v_{\text{wind}}$



Chandra spectra of prototype non-magnetic (zeta Pup, top) and magnetic (θ^1 Ori C, bottom) stars

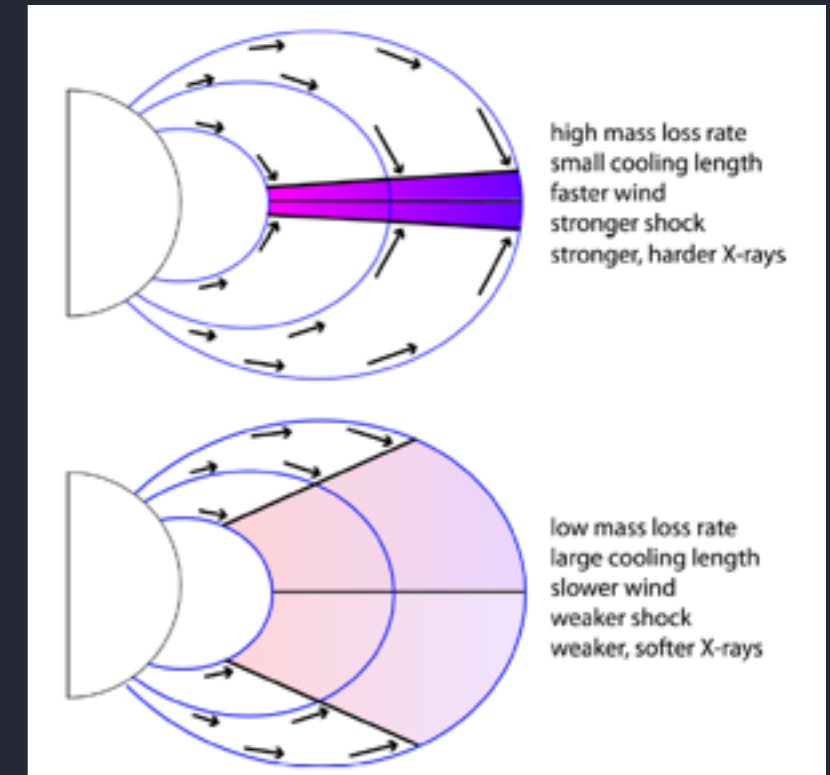
Overall level and hardness of X-ray emission

affected by:

amount of wind material fed into the magnetosphere

efficiency of shock heating (duty cycle of shock build up vs. fall-back/downflow)

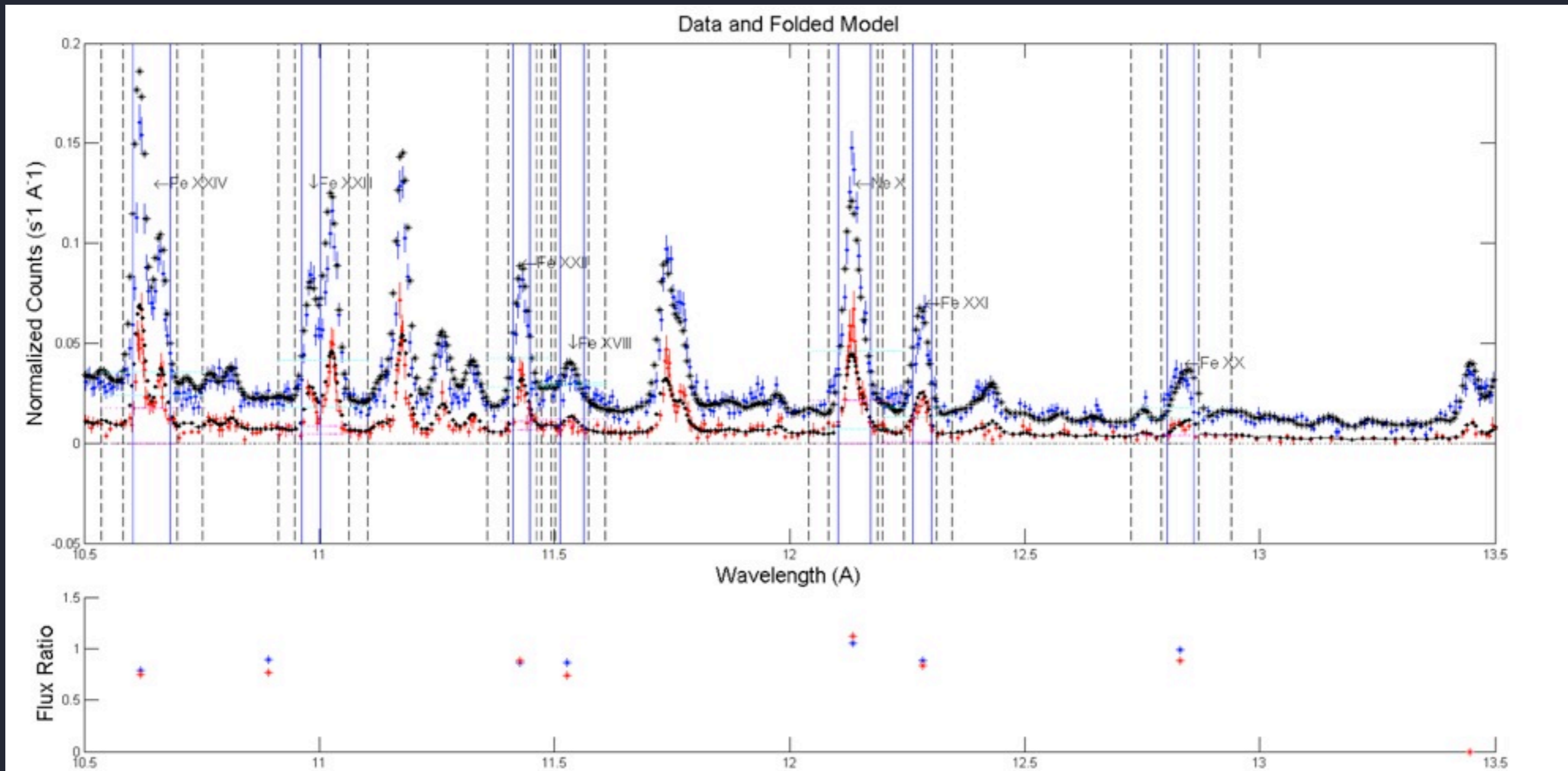
specific kinetic energy: shock velocity (pre-shock wind velocity)



from ud-Doula et al. 2014

traditional approach: spectral modeling

collisional-radiative equilibrium model (APEC): temperature and **emission measure** are free parameters, along with line widths and (potentially) abundances



fit to *Chandra* spectrum

*emission measure: traditional normalization
of X-ray emission spectra*

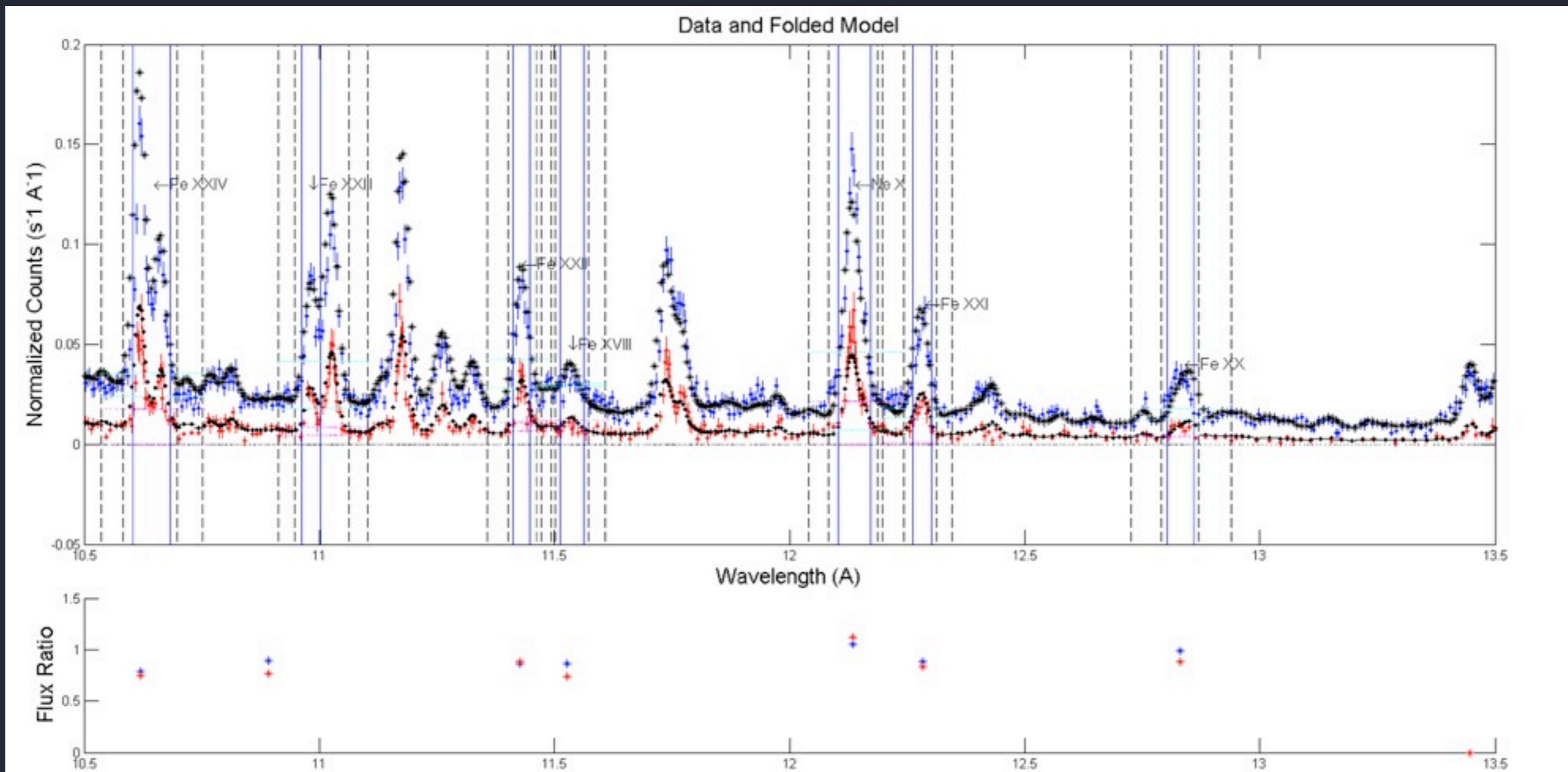
$$\mathcal{E}M \equiv \int n_e n_H dV$$

a DEM, $\phi(\hat{T})$, where

$$\phi(\hat{T}) = n_e n_H \frac{dV}{dT}$$

traditional approach: spectral modeling

zoom-in: black = model; red, blue = data (two grating arrays on *Chandra* produce two spectra, simultaneously)



data - model agreement is quite good

fit to *Chandra* spectrum

Spectral modeling

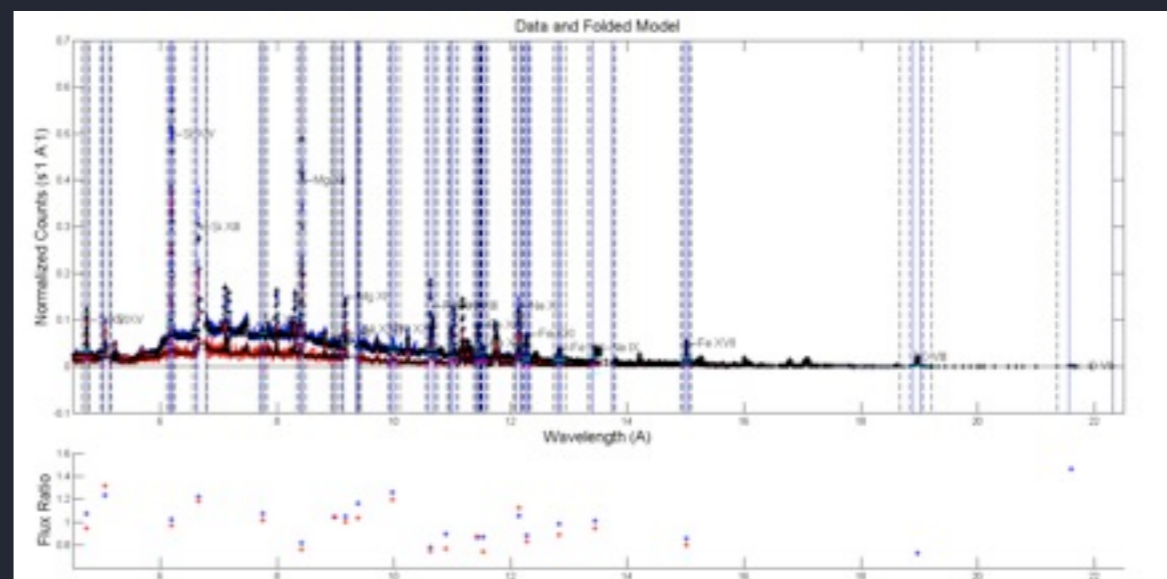
work presented here is preliminary

best-fit model parameters: temperature distribution in the plasma, line widths, absorption

```
=====
Model (bapec<1> + bapec<2> + bapec<3> + bapec<4> + bapec<5> + bapec<6>)TBabs<7>
Source No.: 1 Active/On
Model Model Component Parameter Unit Value
par comp
  1 1 bapec kT keV 0.200000 frozen
  2 1 bapec Abundanc 1.00000 frozen
  3 1 bapec Redshift 0.0 frozen
  4 1 bapec Velocity km/s 290.281 +/- 2.52376
  5 1 bapec norm 1.11264E-02 +/- 5.74059E-04
  6 2 bapec kT keV 0.400000 frozen
  7 2 bapec Abundanc 1.00000 frozen
  8 2 bapec Redshift 0.0 frozen
  9 2 bapec Velocity km/s 290.281 = 1.0*4
 10 2 bapec norm 2.00501E-03 +/- 1.13754E-04
 11 3 bapec kT keV 0.800000 frozen
 12 3 bapec Abundanc 1.00000 frozen
 13 3 bapec Redshift 0.0 frozen
 14 3 bapec Velocity km/s 290.281 = 1.0*4
 15 3 bapec norm 5.02117E-03 +/- 9.06196E-05
 16 4 bapec kT keV 1.60000 frozen
 17 4 bapec Abundanc 1.00000 frozen
 18 4 bapec Redshift 0.0 frozen
 19 4 bapec Velocity km/s 290.281 = 1.0*4
 20 4 bapec norm 7.56200E-03 +/- 1.89407E-04
 21 5 bapec kT keV 3.20000 frozen
 22 5 bapec Abundanc 1.00000 frozen
 23 5 bapec Redshift 0.0 frozen
 24 5 bapec Velocity km/s 290.281 = 1.0*4
 25 5 bapec norm 2.07156E-02 +/- 4.52703E-04
 26 6 bapec kT keV 6.40000 frozen
 27 6 bapec Abundanc 1.00000 frozen
 28 6 bapec Redshift 0.0 frozen
 29 6 bapec Velocity km/s 290.281 = 1.0*4
 30 6 bapec norm 2.45517E-03 +/- 3.00636E-04
 31 7 TBabs nH 10^22 0.616796 +/- 4.19245E-03
=====

Fit statistic : C-Statistic = 13812.32 using 4807 PHA bins and 4799 degrees of freedom.
Warning: cstat statistic is only valid for Poisson data.
Source file is not Poisson

Test statistic : Chi-Squared = 9258.43 using 4807 PHA bins.
Reduced chi-squared = 1.92924 for 4799 degrees of freedom
Null hypothesis probability = 2.369129e-286
```



fit to Chandra spectrum

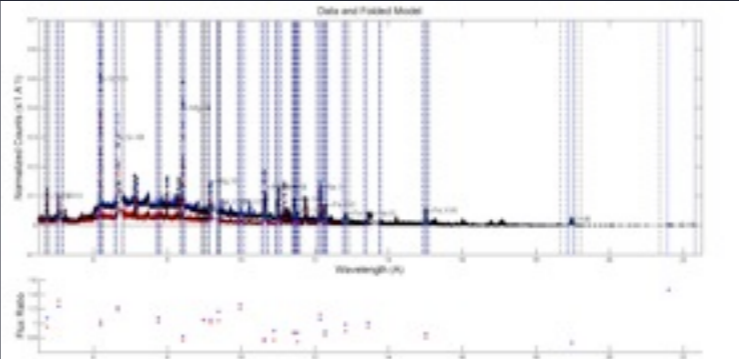
line widths ~ 300 km/s

ISM column density ~ $6 \times 10^{21} \text{ cm}^{-2}$
(maybe a bit more than ISM)

Spectral modeling

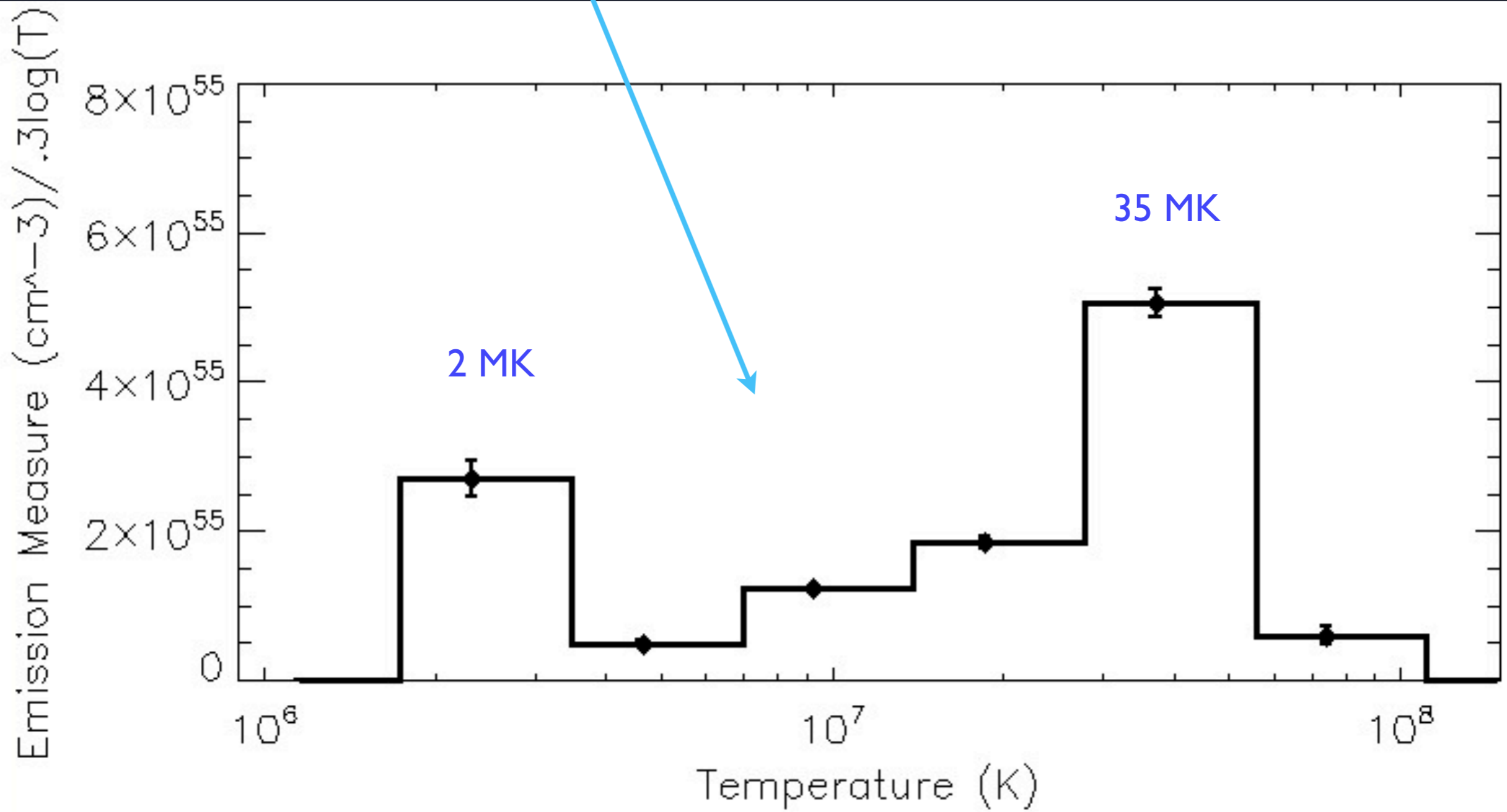
temperature distribution

from the APEC spectral fit



fit to Chandra spectrum

| id | name | type | value | unit | lower | upper |
|-----|-------|-------|---------|------|-------|-------|
| 1 | Norm | norm | 1.00000 | | | |
| 2 | tbabs | tbabs | 1.00000 | | | |
| 3 | tbabs | tbabs | 1.00000 | | | |
| 4 | tbabs | tbabs | 1.00000 | | | |
| 5 | tbabs | tbabs | 1.00000 | | | |
| 6 | tbabs | tbabs | 1.00000 | | | |
| 7 | tbabs | tbabs | 1.00000 | | | |
| 8 | tbabs | tbabs | 1.00000 | | | |
| 9 | tbabs | tbabs | 1.00000 | | | |
| 10 | tbabs | tbabs | 1.00000 | | | |
| 11 | tbabs | tbabs | 1.00000 | | | |
| 12 | tbabs | tbabs | 1.00000 | | | |
| 13 | tbabs | tbabs | 1.00000 | | | |
| 14 | tbabs | tbabs | 1.00000 | | | |
| 15 | tbabs | tbabs | 1.00000 | | | |
| 16 | tbabs | tbabs | 1.00000 | | | |
| 17 | tbabs | tbabs | 1.00000 | | | |
| 18 | tbabs | tbabs | 1.00000 | | | |
| 19 | tbabs | tbabs | 1.00000 | | | |
| 20 | tbabs | tbabs | 1.00000 | | | |
| 21 | tbabs | tbabs | 1.00000 | | | |
| 22 | tbabs | tbabs | 1.00000 | | | |
| 23 | tbabs | tbabs | 1.00000 | | | |
| 24 | tbabs | tbabs | 1.00000 | | | |
| 25 | tbabs | tbabs | 1.00000 | | | |
| 26 | tbabs | tbabs | 1.00000 | | | |
| 27 | tbabs | tbabs | 1.00000 | | | |
| 28 | tbabs | tbabs | 1.00000 | | | |
| 29 | tbabs | tbabs | 1.00000 | | | |
| 30 | tbabs | tbabs | 1.00000 | | | |
| 31 | tbabs | tbabs | 1.00000 | | | |
| 32 | tbabs | tbabs | 1.00000 | | | |
| 33 | tbabs | tbabs | 1.00000 | | | |
| 34 | tbabs | tbabs | 1.00000 | | | |
| 35 | tbabs | tbabs | 1.00000 | | | |
| 36 | tbabs | tbabs | 1.00000 | | | |
| 37 | tbabs | tbabs | 1.00000 | | | |
| 38 | tbabs | tbabs | 1.00000 | | | |
| 39 | tbabs | tbabs | 1.00000 | | | |
| 40 | tbabs | tbabs | 1.00000 | | | |
| 41 | tbabs | tbabs | 1.00000 | | | |
| 42 | tbabs | tbabs | 1.00000 | | | |
| 43 | tbabs | tbabs | 1.00000 | | | |
| 44 | tbabs | tbabs | 1.00000 | | | |
| 45 | tbabs | tbabs | 1.00000 | | | |
| 46 | tbabs | tbabs | 1.00000 | | | |
| 47 | tbabs | tbabs | 1.00000 | | | |
| 48 | tbabs | tbabs | 1.00000 | | | |
| 49 | tbabs | tbabs | 1.00000 | | | |
| 50 | tbabs | tbabs | 1.00000 | | | |
| 51 | tbabs | tbabs | 1.00000 | | | |
| 52 | tbabs | tbabs | 1.00000 | | | |
| 53 | tbabs | tbabs | 1.00000 | | | |
| 54 | tbabs | tbabs | 1.00000 | | | |
| 55 | tbabs | tbabs | 1.00000 | | | |
| 56 | tbabs | tbabs | 1.00000 | | | |
| 57 | tbabs | tbabs | 1.00000 | | | |
| 58 | tbabs | tbabs | 1.00000 | | | |
| 59 | tbabs | tbabs | 1.00000 | | | |
| 60 | tbabs | tbabs | 1.00000 | | | |
| 61 | tbabs | tbabs | 1.00000 | | | |
| 62 | tbabs | tbabs | 1.00000 | | | |
| 63 | tbabs | tbabs | 1.00000 | | | |
| 64 | tbabs | tbabs | 1.00000 | | | |
| 65 | tbabs | tbabs | 1.00000 | | | |
| 66 | tbabs | tbabs | 1.00000 | | | |
| 67 | tbabs | tbabs | 1.00000 | | | |
| 68 | tbabs | tbabs | 1.00000 | | | |
| 69 | tbabs | tbabs | 1.00000 | | | |
| 70 | tbabs | tbabs | 1.00000 | | | |
| 71 | tbabs | tbabs | 1.00000 | | | |
| 72 | tbabs | tbabs | 1.00000 | | | |
| 73 | tbabs | tbabs | 1.00000 | | | |
| 74 | tbabs | tbabs | 1.00000 | | | |
| 75 | tbabs | tbabs | 1.00000 | | | |
| 76 | tbabs | tbabs | 1.00000 | | | |
| 77 | tbabs | tbabs | 1.00000 | | | |
| 78 | tbabs | tbabs | 1.00000 | | | |
| 79 | tbabs | tbabs | 1.00000 | | | |
| 80 | tbabs | tbabs | 1.00000 | | | |
| 81 | tbabs | tbabs | 1.00000 | | | |
| 82 | tbabs | tbabs | 1.00000 | | | |
| 83 | tbabs | tbabs | 1.00000 | | | |
| 84 | tbabs | tbabs | 1.00000 | | | |
| 85 | tbabs | tbabs | 1.00000 | | | |
| 86 | tbabs | tbabs | 1.00000 | | | |
| 87 | tbabs | tbabs | 1.00000 | | | |
| 88 | tbabs | tbabs | 1.00000 | | | |
| 89 | tbabs | tbabs | 1.00000 | | | |
| 90 | tbabs | tbabs | 1.00000 | | | |
| 91 | tbabs | tbabs | 1.00000 | | | |
| 92 | tbabs | tbabs | 1.00000 | | | |
| 93 | tbabs | tbabs | 1.00000 | | | |
| 94 | tbabs | tbabs | 1.00000 | | | |
| 95 | tbabs | tbabs | 1.00000 | | | |
| 96 | tbabs | tbabs | 1.00000 | | | |
| 97 | tbabs | tbabs | 1.00000 | | | |
| 98 | tbabs | tbabs | 1.00000 | | | |
| 99 | tbabs | tbabs | 1.00000 | | | |
| 100 | tbabs | tbabs | 1.00000 | | | |



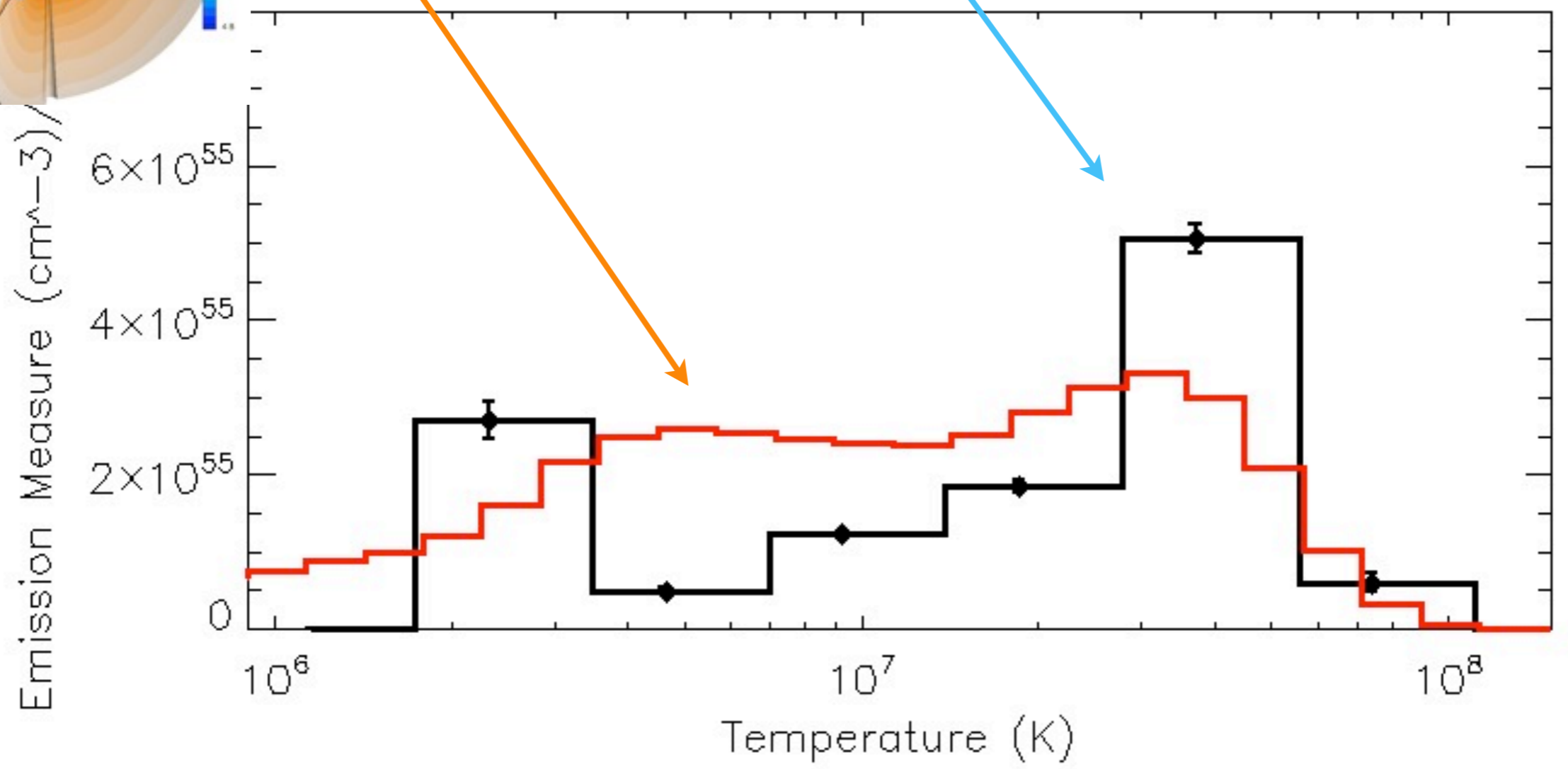
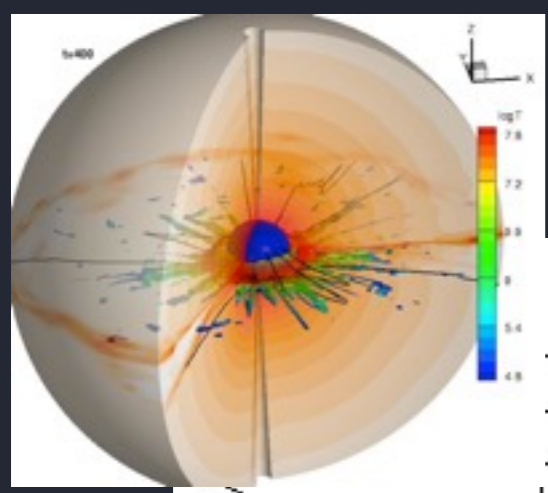
Spectral modeling

The overall amount of hot plasma produced in the MHD simulations is in good agreement with the data (but a **factor of 3 too high**); the temperature distribution is in good agreement, too.

Emission Measure (EM) distribution

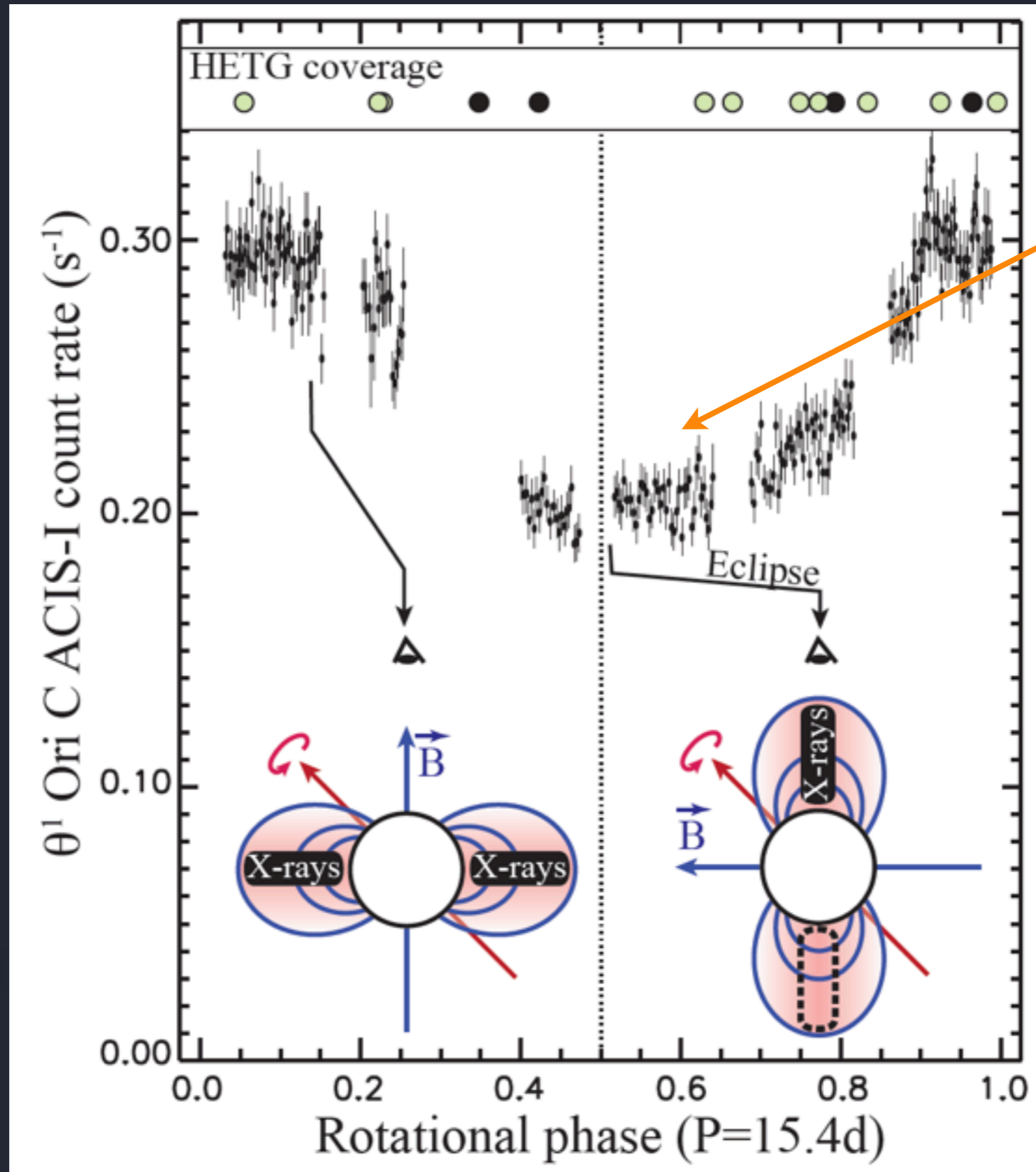
from 3-D MHD simulation

APEC spectral fit



rotationally modulated X-ray variability

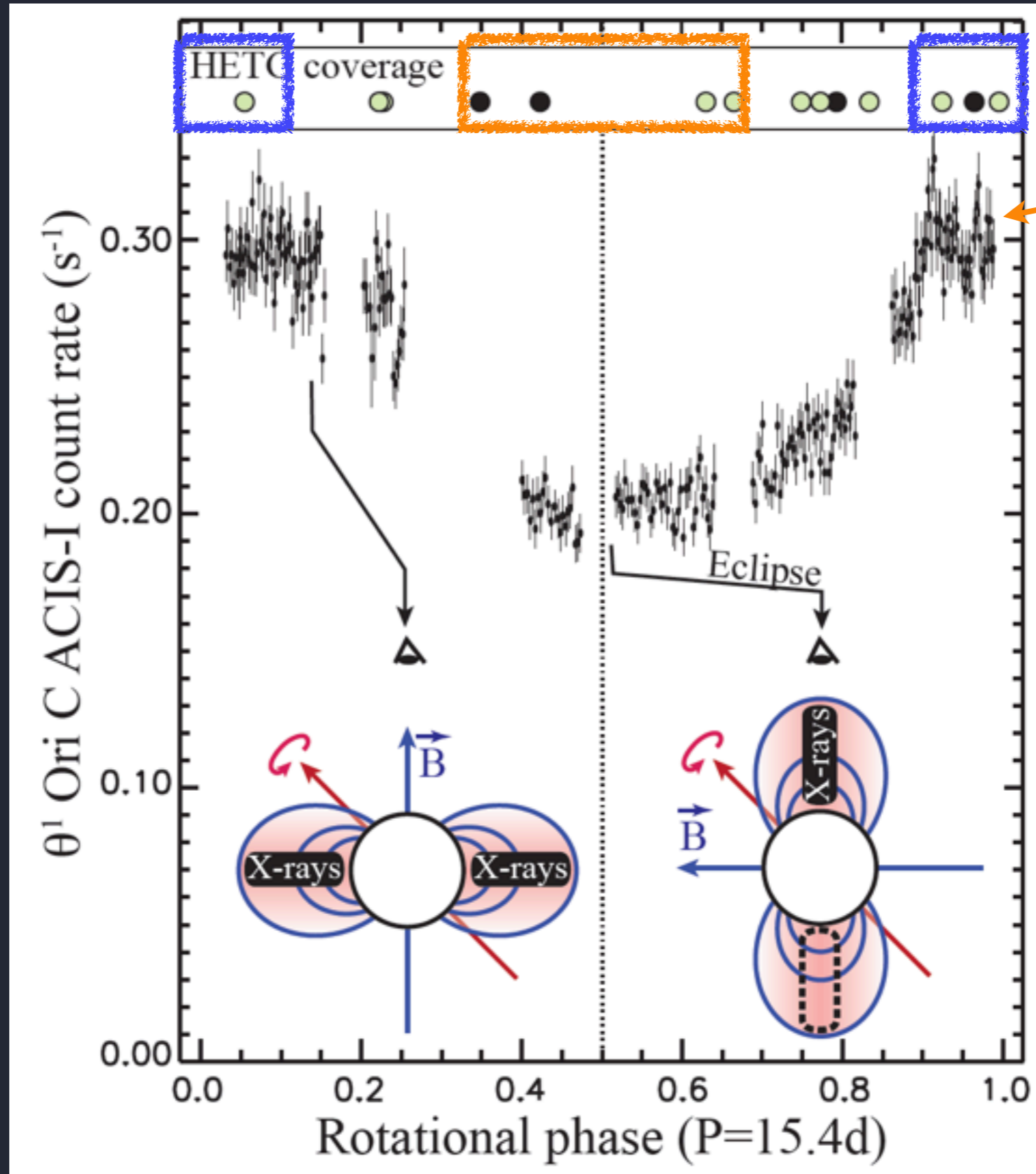
X-ray light curve: phase coverage: new data (11 new pointings (N. Schulz, PI) to supplement 4 in Gagne et al. 2005)



X-rays:
occultation
causes the
magneto-
spheric
eclipse

work presented here
is preliminary

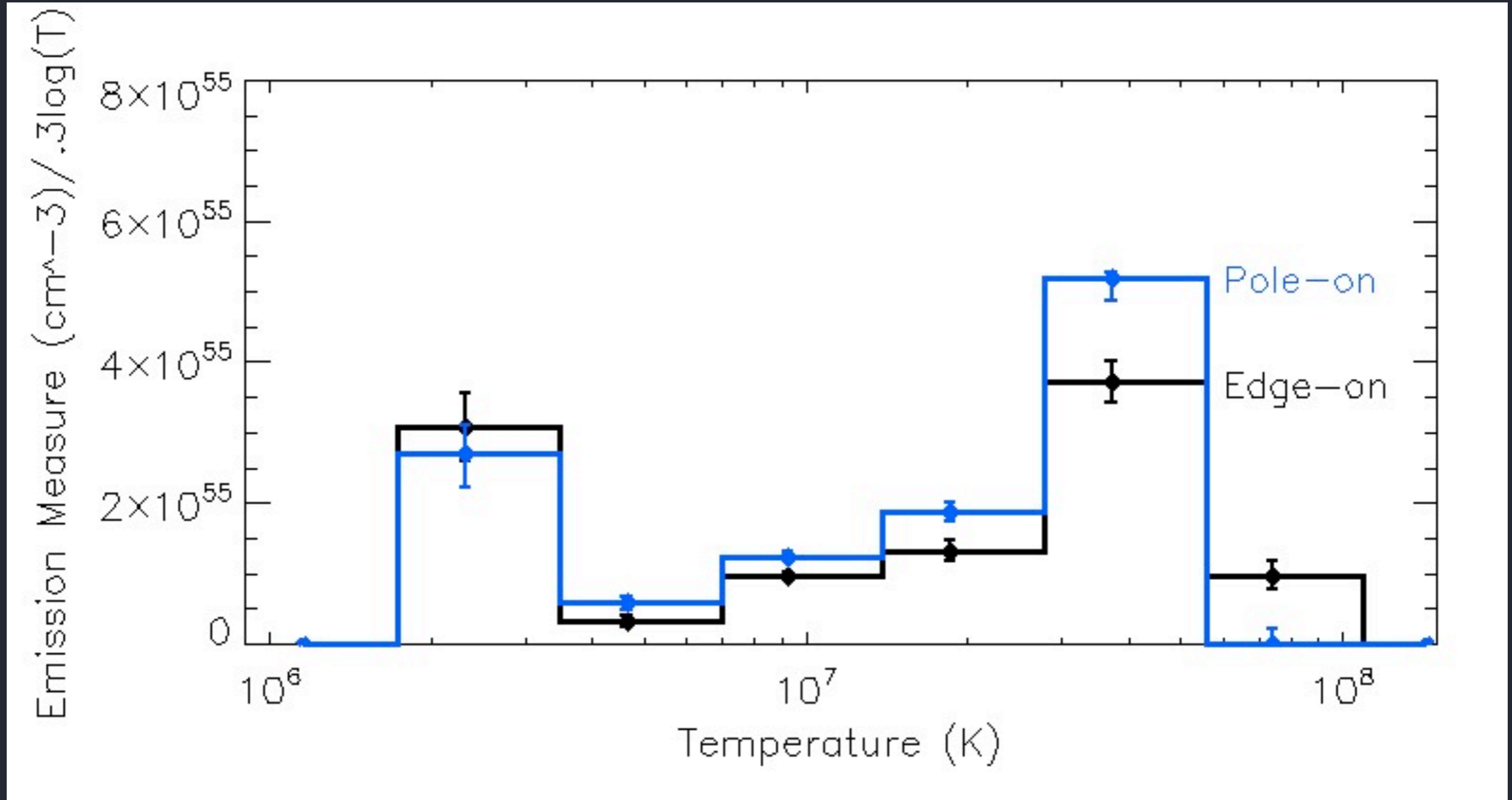
Look at the most pole-on and most edge-on observations



X-rays:
occultation
causes the
magneto-
spheric
eclipse

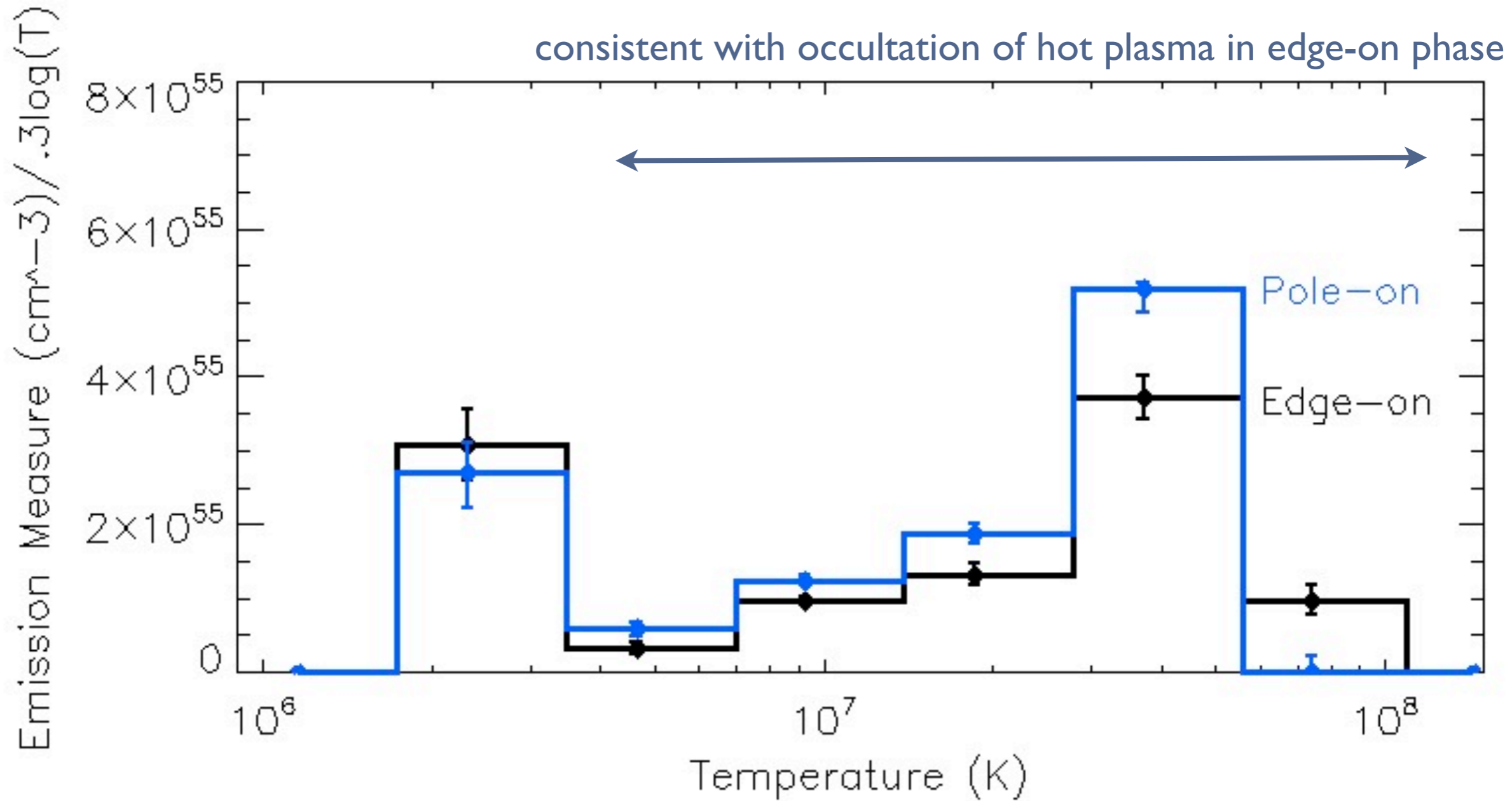
Spectral modeling: coadded 4 observations ea. pole-on and edge-on

emission measure distributions



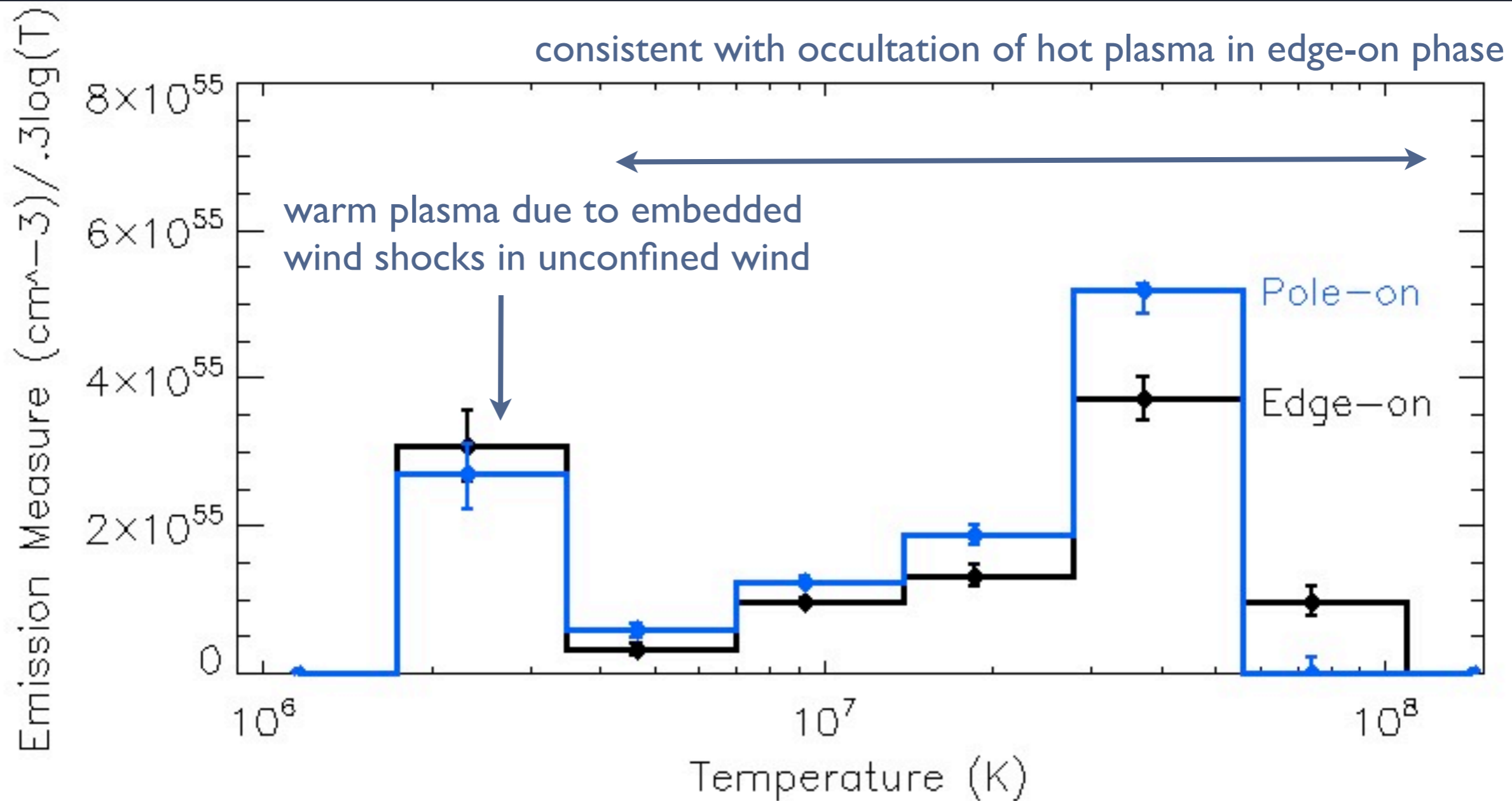
Spectral modeling: coadded 4 observations ea. pole-on and edge-on

emission measure distributions



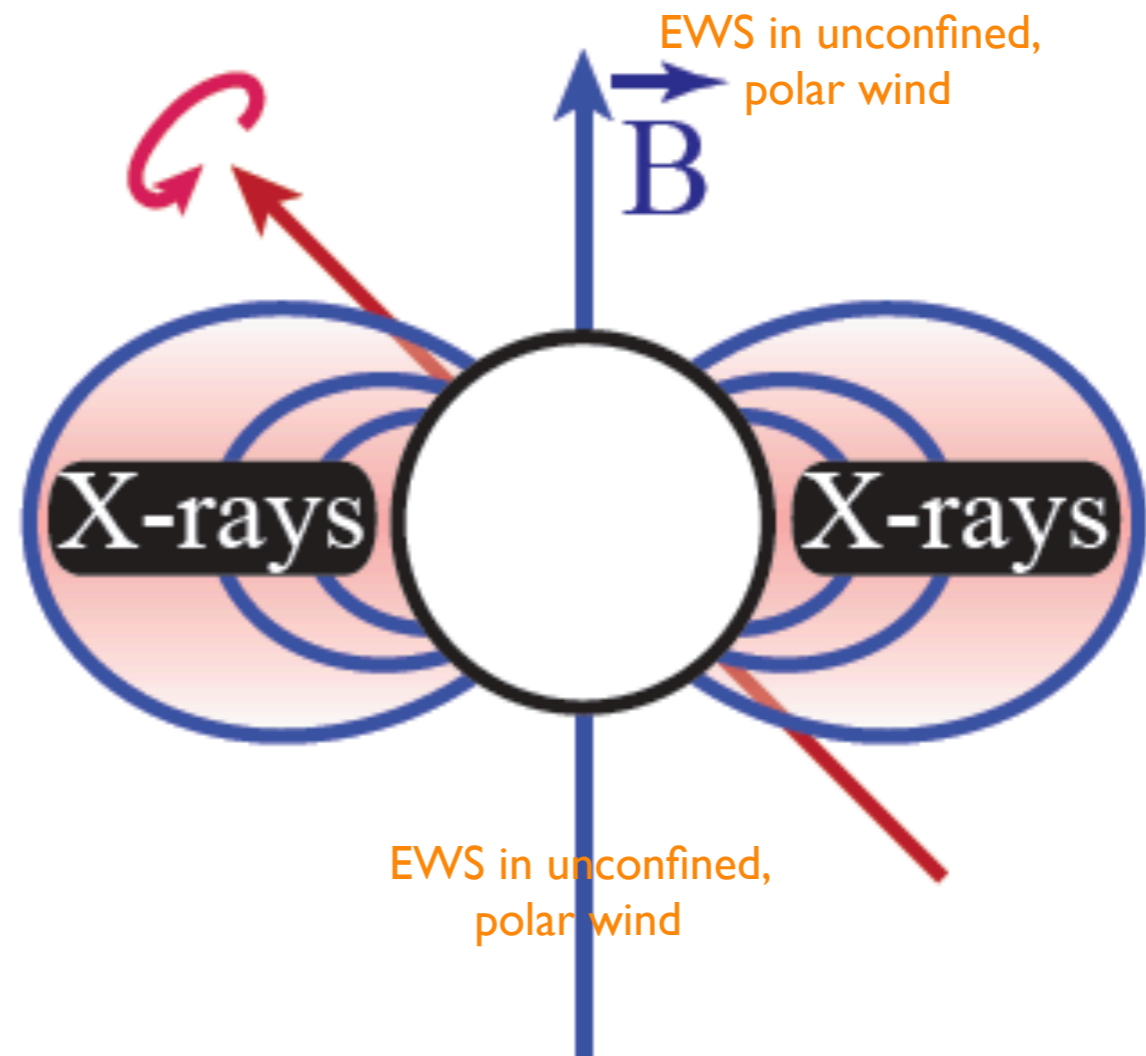
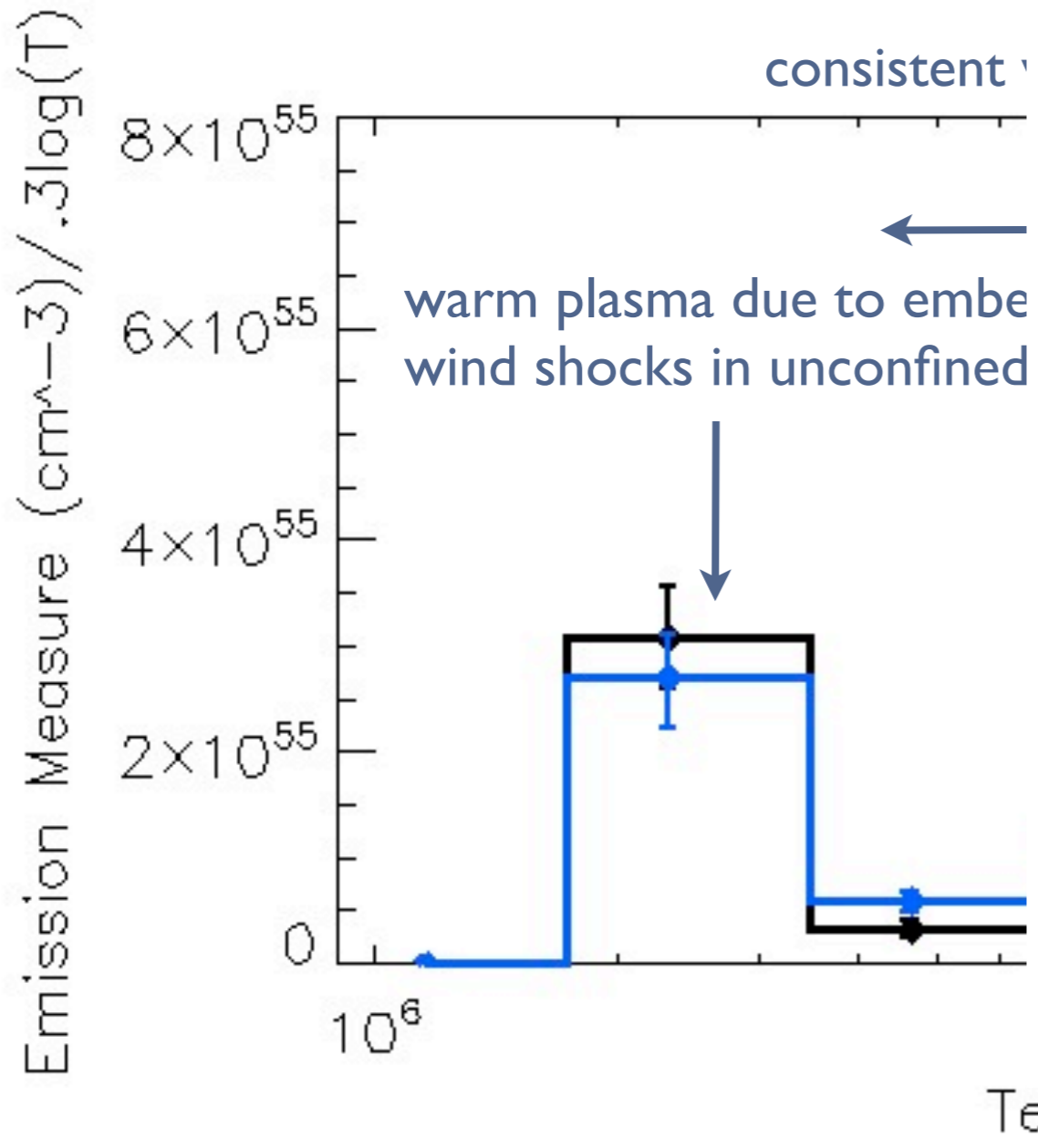
Spectral modeling: coadded 4 observations ea. pole-on and edge-on

emission measure distributions



Spectral modeling: coadded 4 observations ea. pole-on and edge-on

emission measure distributions



A different way to extract information from the X-ray spectrum

DEM (temperature distribution) tells us about the heating and cooling's combined effects

MCWS X-ray production physics and models are fundamentally about the heating

Because the cooling is primarily radiative, we can in some sense correct for it

THE ASTROPHYSICAL JOURNAL, 788:90 (21pp), 2014 June 10

doi:10.1088/0004-637X/788/1/90

© 2014. The American Astronomical Society. All rights reserved. Printed in the U.S.A.

THERMAL X-RAY SPECTRAL TOOLS. I. PARAMETERIZING IMPULSIVE X-RAY HEATING WITH A CUMULATIVE INITIAL TEMPERATURE (CIT) DISTRIBUTION

KENNETH G. GAYLEY

Department of Physics and Astronomy, University of Iowa, Iowa City, IA 52242, USA

Received 2014 January 26; accepted 2014 April 15; published 2014 May 27

ABSTRACT

In collisional ionization equilibrium, the X-ray spectrum from a plasma depends on the differential emission measure (DEM), distributed over temperature. Due to the well-known ill conditioning problem, no precisely resolved DEM can be inverted directly from the spectrum, so often only a gross parameterization of the DEM is used to approximate the data, in hopes that the parameterization can provide useful model-independent constraints on the heating process. However, ill conditioning also introduces ambiguity into the various different parameterizations that could approximate the data, which may spoil the perceived advantages of model independence. Thus, this paper instead suggests a single parameterization for both the heating mechanism and the X-ray sources, based on a model of impulsive heating followed by radiative cooling. This approach is similar to a “cooling flow” approach but allows injection at multiple initial temperatures and applies even when the steady state is a distribution of different shock strengths, as for a standing shock with a range of obliquities, or for embedded stochastic shocks that are only steady in a statistical sense. This produces an alternative parameterization for X-ray spectra that is especially streamlined for higher density plasmas with efficient radiative cooling and minimal thermal conduction and mixing. The method also provides some internal consistency checks on the validity of its assumptions. A heuristic general version is then applied over a wide range of astrophysical applications to schematically explore potential alternative models for these phenomena.

Key words: line: formation – methods: analytical – radiation mechanisms: thermal – techniques: spectroscopic – X-rays: general

Measuring the shock-heating rate in the winds of O stars using X-ray line spectra

David H. Cohen,^{1*} Zequn Li,¹ Kenneth G. Gayley,² Stanley P. Owocki,³
Jon O. Sundqvist,^{3,4} Véronique Petit,^{3,5} Maurice A. Leutenegger^{6,7}

¹*Swarthmore College, Department of Physics and Astronomy, Swarthmore, PA 19081, USA*

²*University of Iowa, Department of Physics and Astronomy, Iowa City, IA 52242, USA*

³*University of Delaware, Bartol Research Institute, Newark, DE 19716, USA*

⁴*Institut für Astronomie und Astrophysik der Universität München, Scheinerstr. 1, 81679 München, Germany*

⁵*Florida Institute of Technology, Department of Physics and Space Sciences, Melbourne, FL 32901, USA*

⁶*NASA/Goddard Space Flight Center, Code 662, Greenbelt, MD 20771, USA*

⁷*CRESST and University of Maryland, Baltimore County, Baltimore, MD 21250, USA*

new paper applying the Gayley method to non-magnetic O stars with embedded wind shocks: see today's Massive Star News!

ratio of line emissivity to total emissivity: line luminosity “branching ratio”

$$f_\ell(T_s) = \int_0^{T_s} \frac{\Lambda_\ell(T)}{\Lambda(T)} \frac{dT}{T_s}$$

$$\Delta T_\ell \equiv \int_0^\infty \frac{\Lambda_\ell(T)}{\Lambda(T)} dT$$

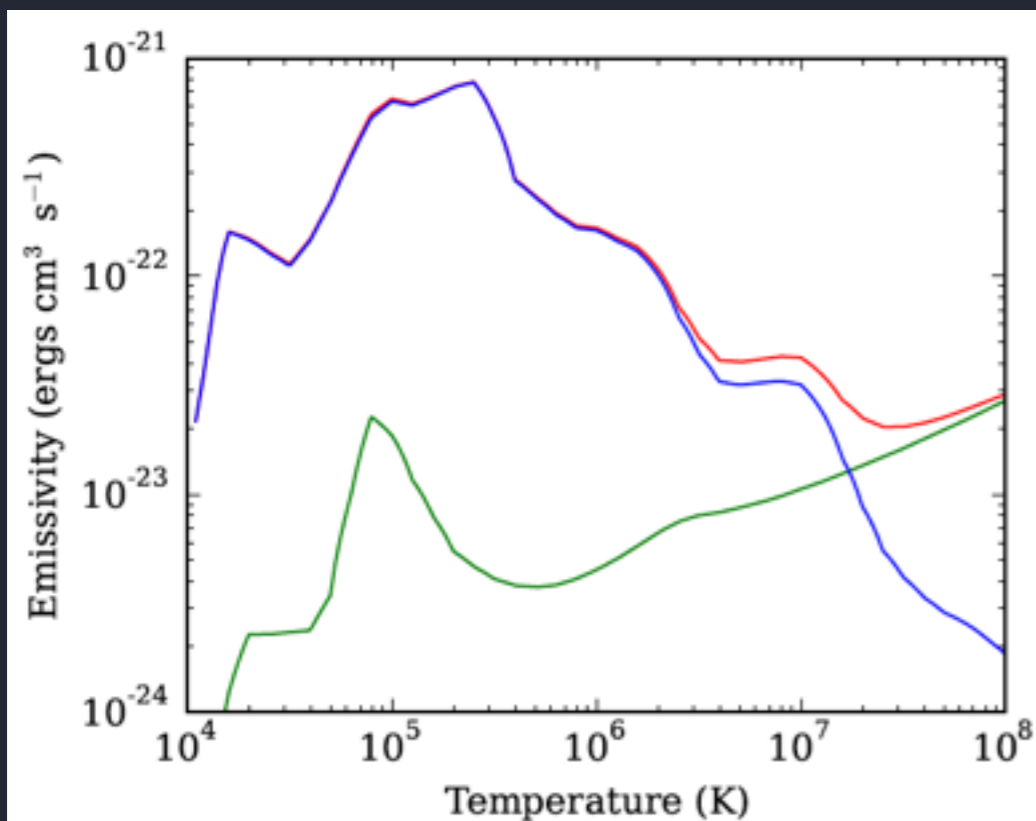
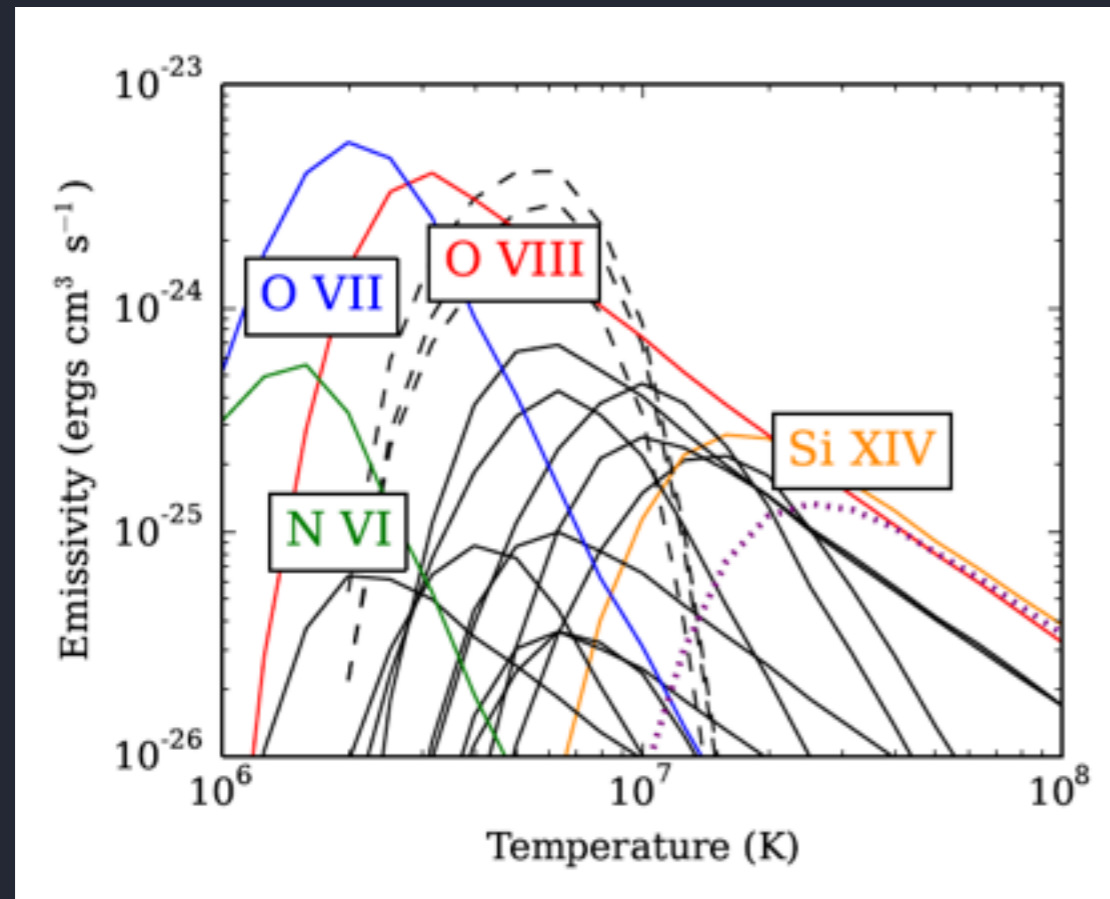


Figure 2. The contribution of all emission lines (blue) to the total radiated power (red), along with the contribution of continuum processes (green).

line luminosity shock heating probability

$$L_\ell = \dot{M} \frac{5k\Delta T_\ell}{2\mu m_p} \bar{N} p(T_\ell)$$

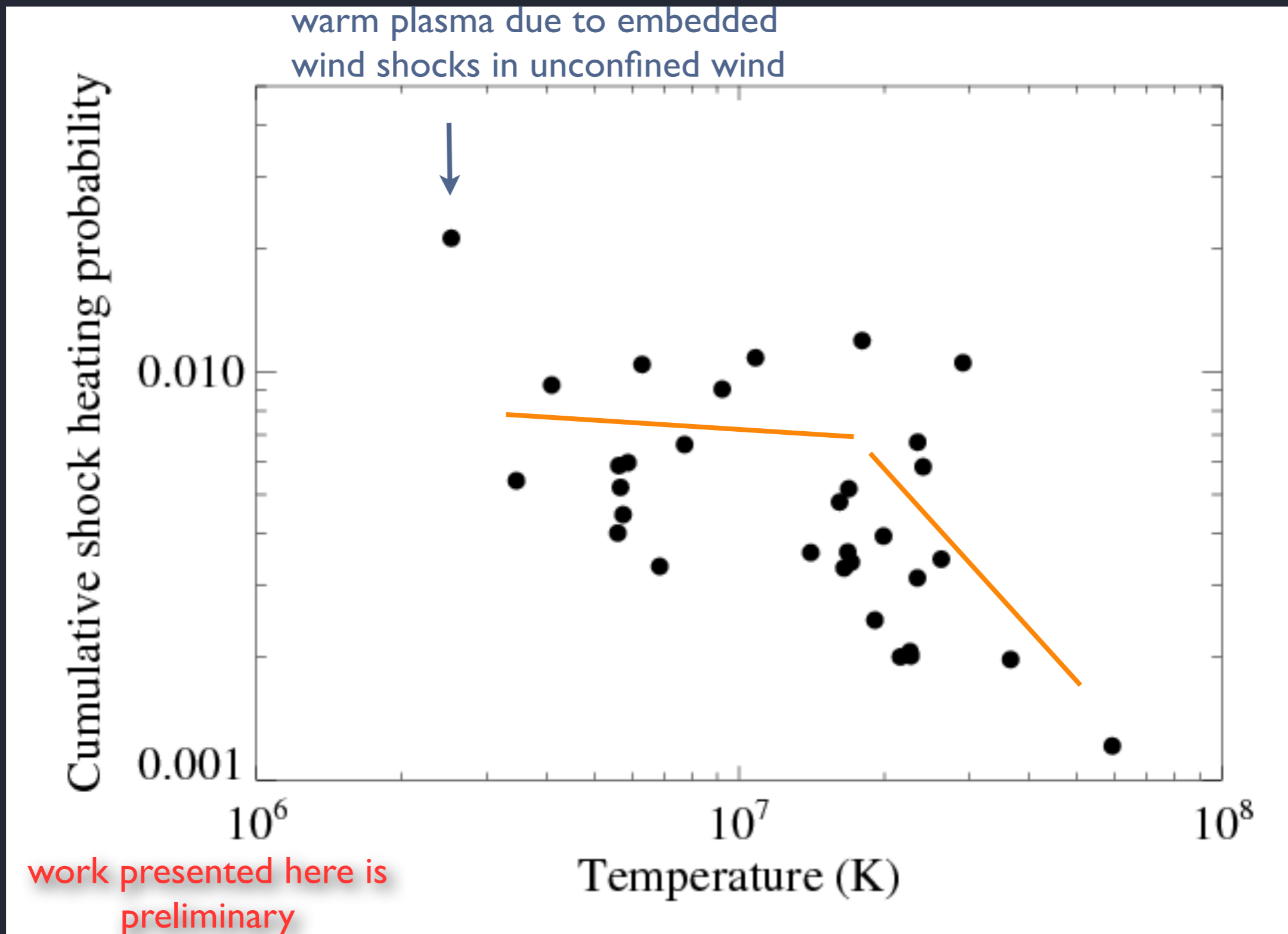
A different way to extract information from the X-ray spectrum

Impulsively heated plasma in the magnetosphere cools radiatively, emitting photons in all lines with characteristic temperatures equal to or less than the shock temperature

The spectral line luminosities naturally provide a **cumulative distribution of shock strengths**

And the heating rate normalization is naturally expressed as a mass-loss rate times a shock efficiency factor

Shock heating rate for each line vs. temperature probed by the line



$N_p(T)$ derived from the Chandra spectrum -
fraction of wind that is shock-heated

$$N_p(T) \sim 0.01 \text{ @ } 20 \text{ or } 30 \text{ MK}$$

assumes $\dot{M} = 5e-7$ ($\sim 1/3$)

must be corrected for fraction of the wind that's confined ($\sim 1/2$)

and corrected for the tilted surface field reduction in mass-flux
($\sim 1/3$)

comparison of the ADM and MHD simulations - duty cycle/efficiency
factor ($\sim 1/5$)

Conclusions:

X-ray properties of θ^1 Ori C remarkably consistent with MHD simulations & analytic MCWS/ADM models

rotational modulation of X-rays consistent with occultation in edge-on view *but* lowest-temperature plasma component due to EWS in polar wind

shock-heating rate measurement: efficiency factor/duty cycle + mass-loss rate

Magnetism and Variability in O Stars

the prophet was right!

Magnetism and variability in O stars

λ

β Cepheus

Cassiopeia

γ

Perseus

ξ

Amsterdam
17-19 September 2014

Extra Slides
(answering audience questions)

Other magnetic O stars: HD 191612 (Of?p)

X-ray luminosity almost as high as θ^1 Ori C

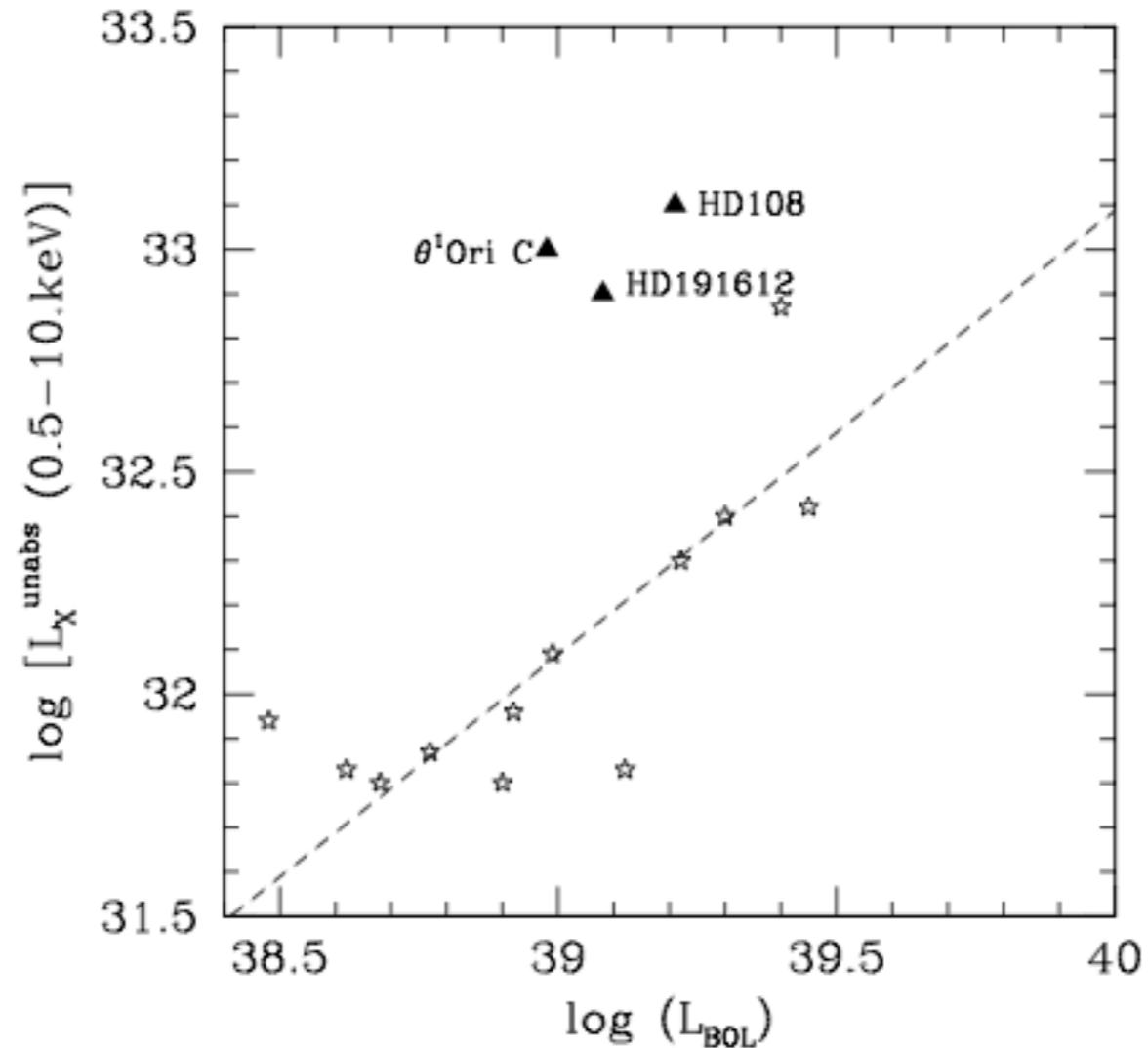
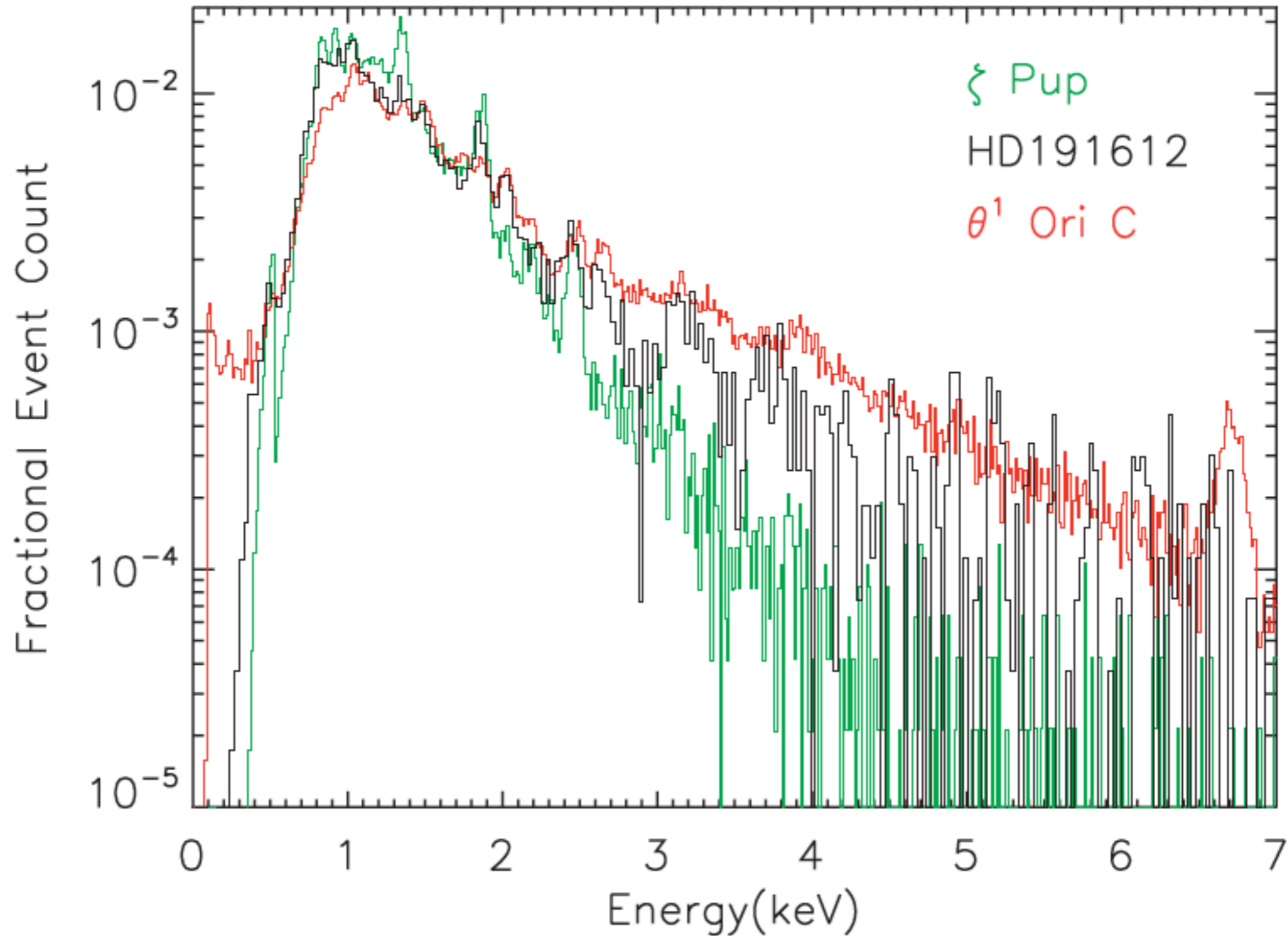


Figure 4. Diagram showing the X-ray luminosity (in erg s^{-1}) versus bolometric luminosity (in erg s^{-1}). The dashed line indicates the typical relation for O stars (from Sana et al. 2006); HD 108, HD 191612 and θ^1 Ori C all lie above it. Asterisks show the position of hot stars in NGC 6231 (Sana et al. 2006) with three outliers: the two objects lying above the line are CW binaries whereas the one lying below is a Wolf-Rayet binary.

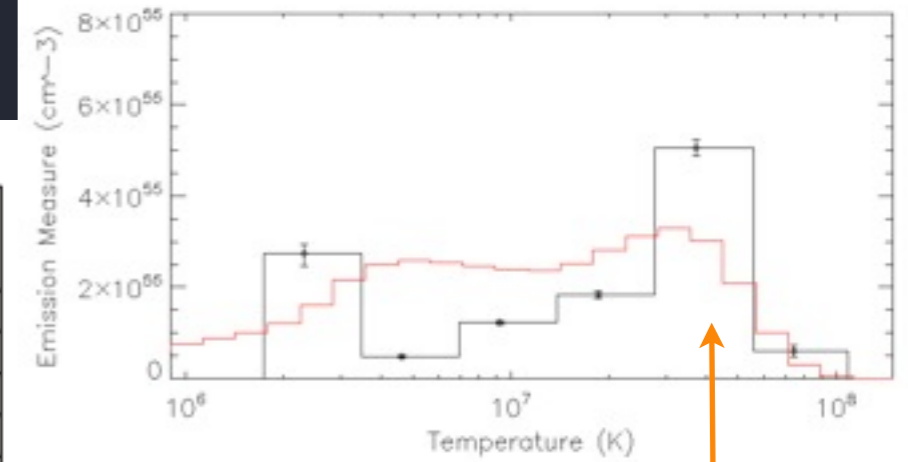
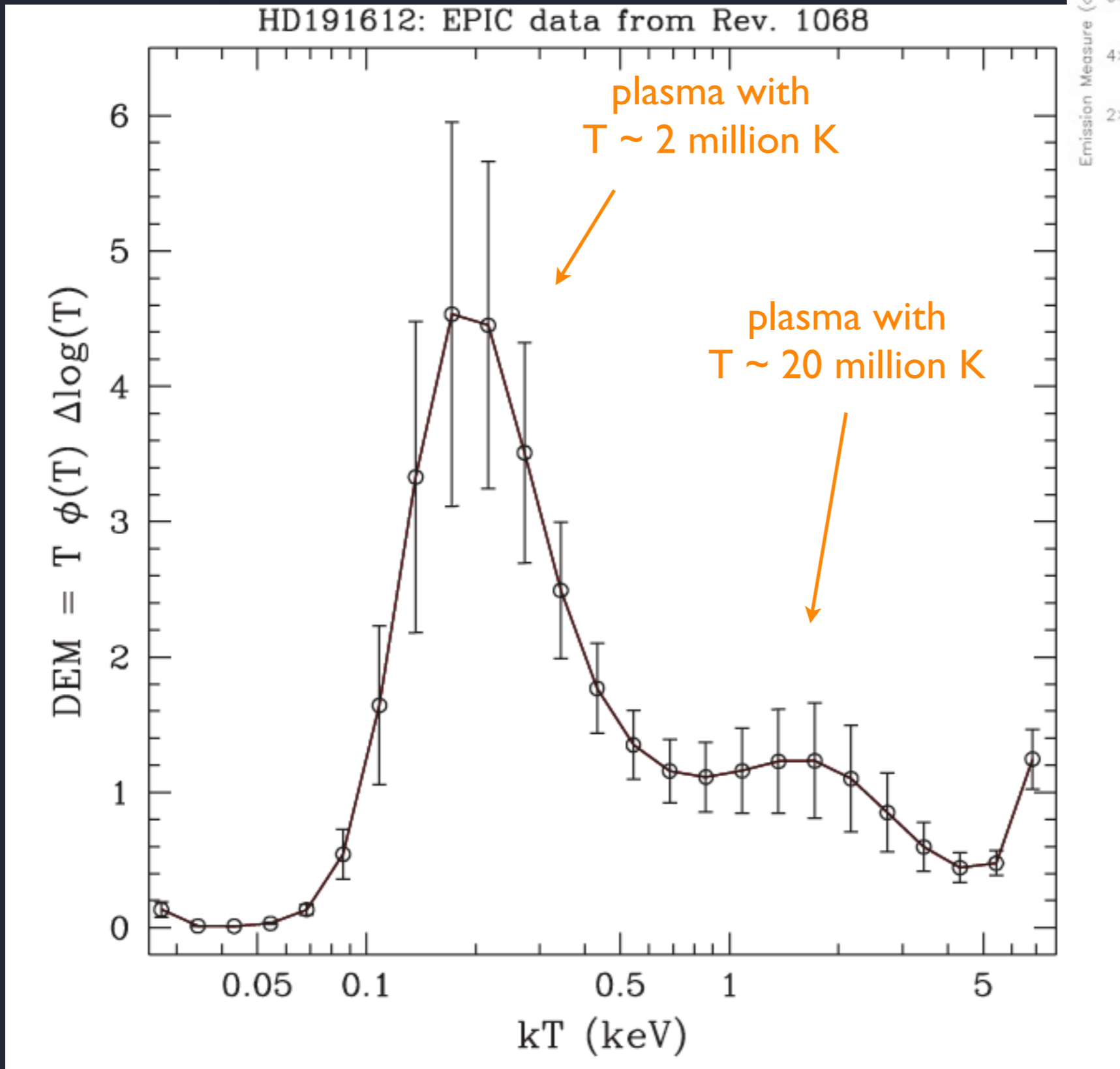
Broadband X-ray spectra: HD 191612

spectrum softer than θ^1 Ori C



HD 191612: some very hot plasma but mostly cooler (few 10^6 K)

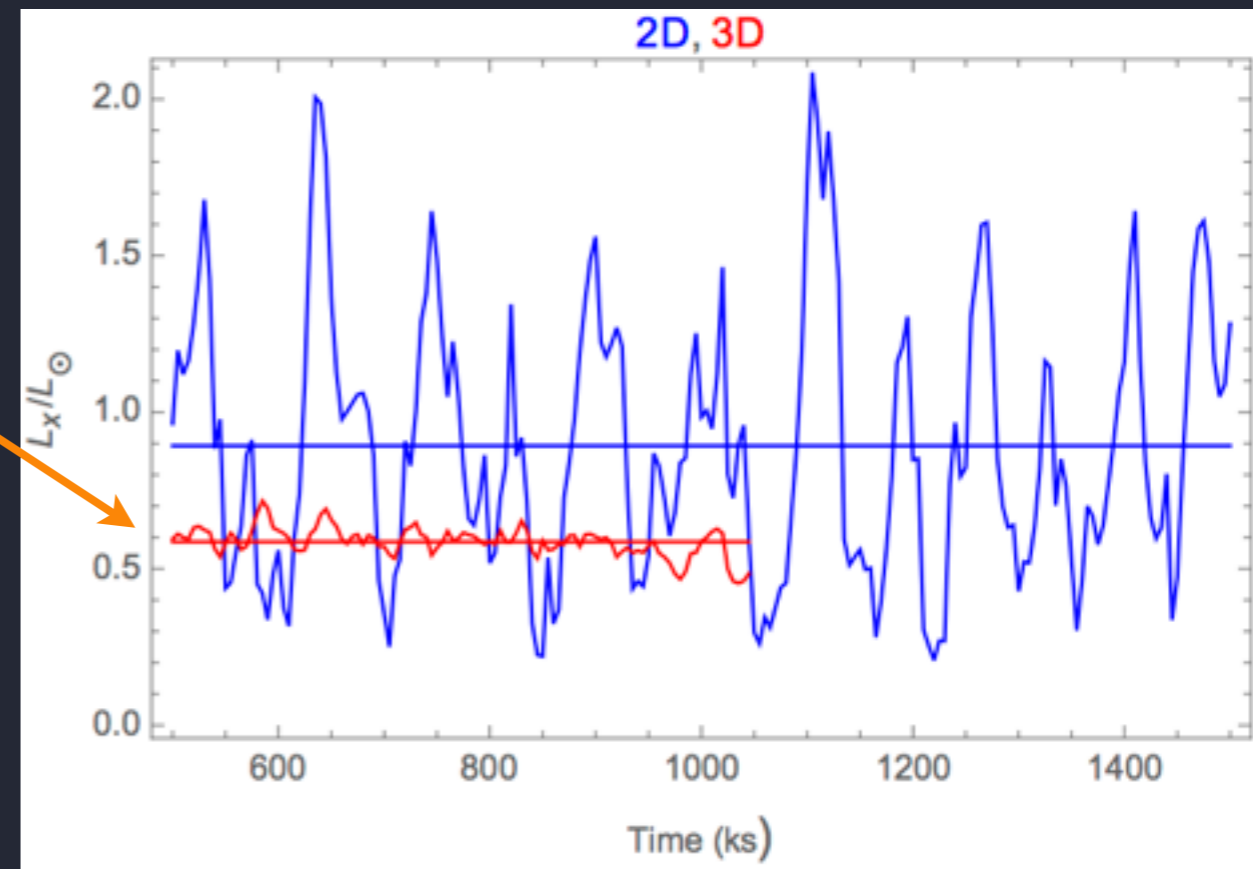
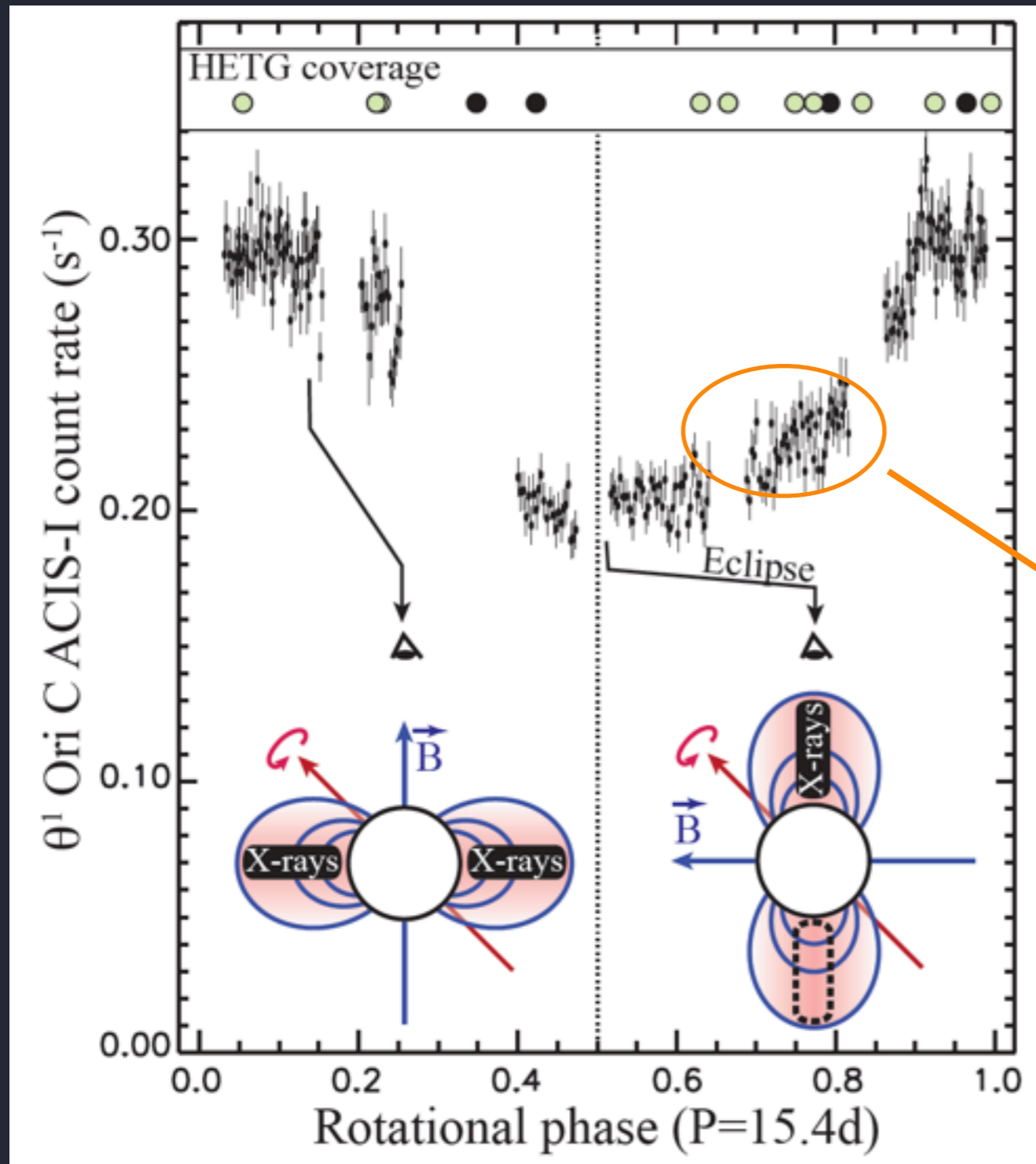
θ^1 Ori C



$kT \sim 3$ keV
(35 million K)

X-ray light curve: focus on the stochastic, short-term variability

variability of $< 10\%$
consistent with 3-D model:
lateral structure



3-D MHD simulation: what about absorption?

optical depth - in ADM model

Analytic Dynamical Magnetosphere 7

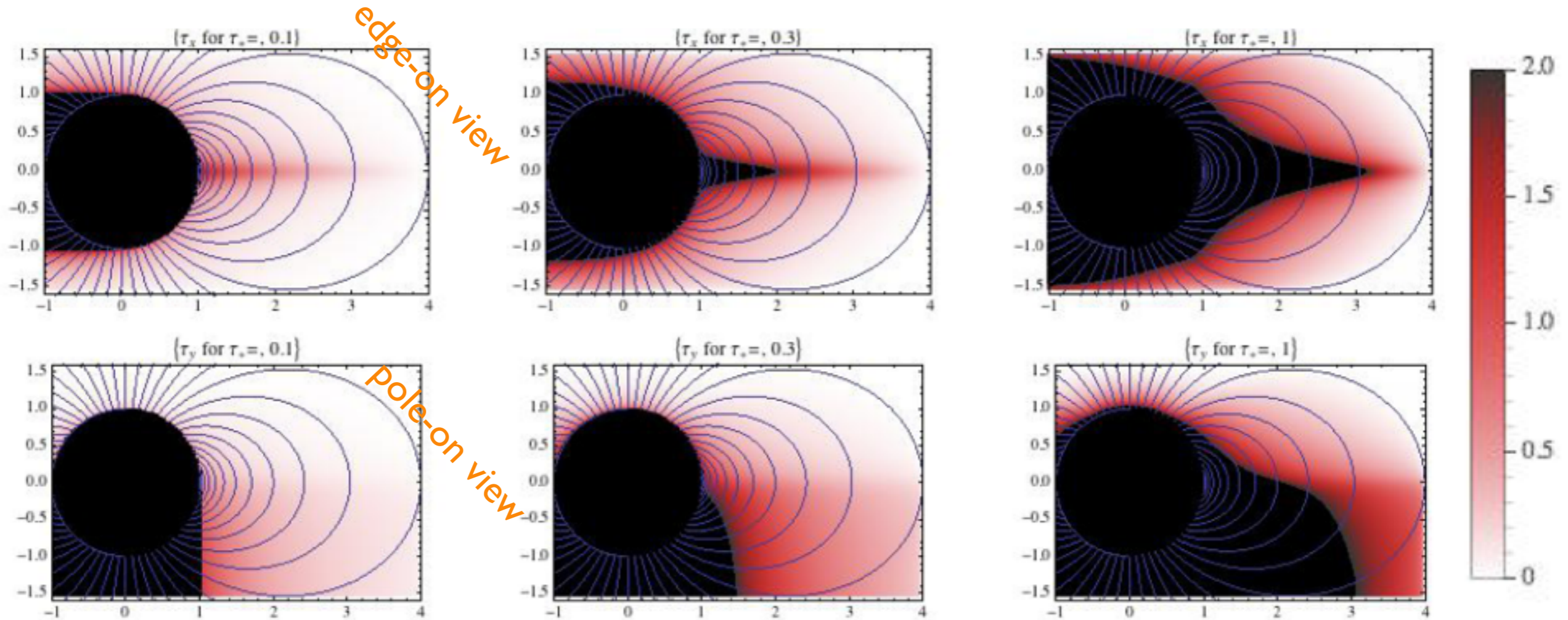
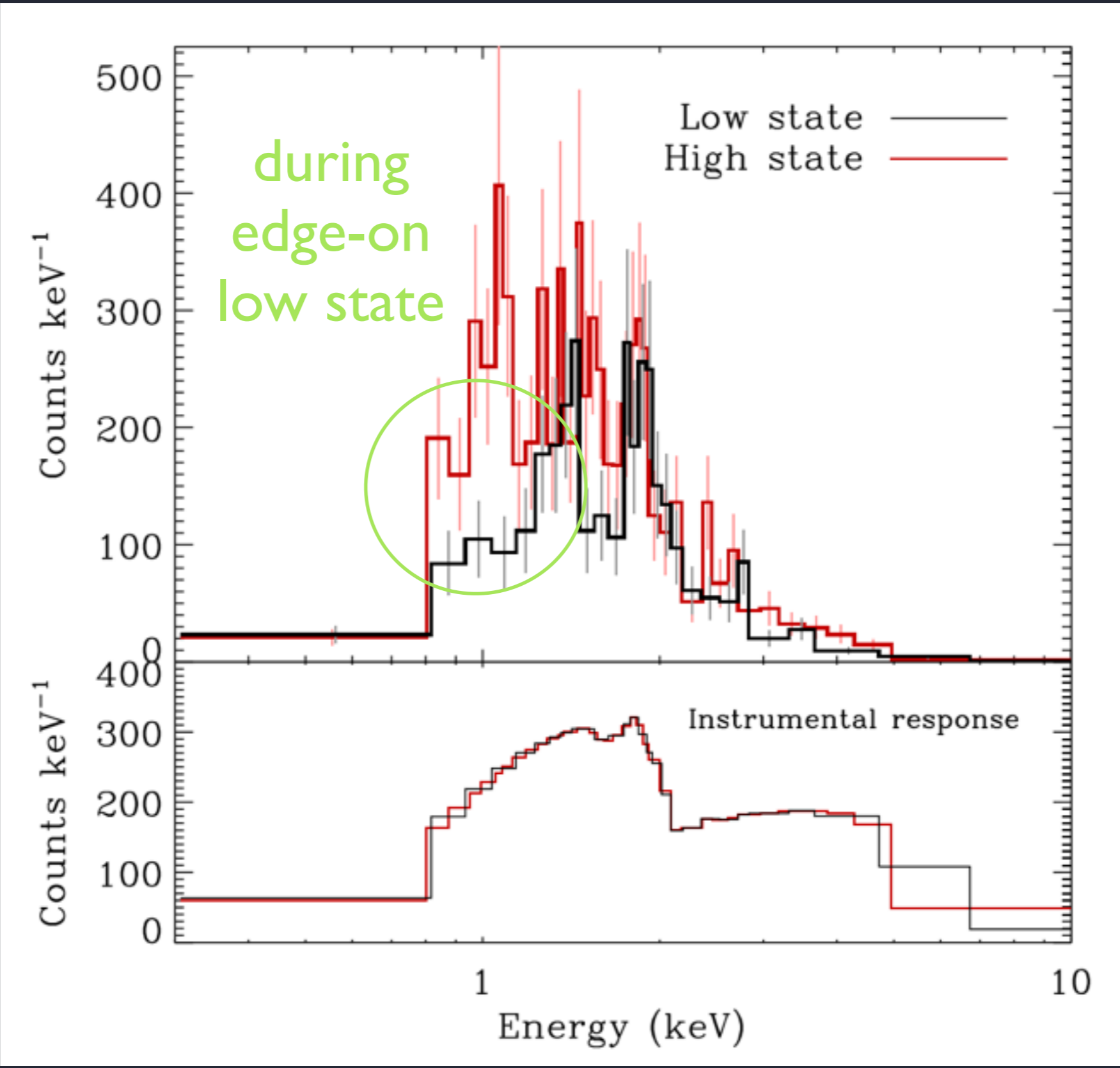


Figure 7. Spatial variation of optical depth for bound-free absorption of X-ray emission by both the cool downflow and wind outflow components of the ADM model, as well as by occultation of the opaque star. The top row shows results for a distant observer to the right, with an equator-on view, while the bottom row is for an observer at the top, with a pole-on view. The model assumes an apex smoothing length $h = 0.1R_*$, and a terminal speed $V_\infty = 3v_e$ for a corresponding unmagnetized wind. The left, middle and right columns show cases with a corresponding wind optical depth $\tau_* = 0.1, 0.3$ and 1 .

Spectral signature of absorption in NGC 1624-2

Of?p with giant magnetosphere



from V. Petit